CLIMATIC AND LACUSTRINE MORPHOMETRIC CONTROLS OF DIATOM PALEOPRODUCTIVITY IN A TROPICAL ANDEAN LAKE

Bao, R.[1*]; Hernández, A.[2]; Sáez, A.[3]; Giralt, S.[4]; Prego, R.[5]; Pueyo, J.J.[3]; Moreno, A.[6] and Valero-Garcés, B. L.[6]

[1]Centro de Investigacións Científicas Avanzadas (CICA), Facultade de Ciencias, Universidade da Coruña, 15071 A Coruña, Spain

[2]Instituto Dom Luiz (IDL), Faculdade de Ciências, Universidade de Lisboa, Lisbon 1749-016, Portugal

[3]Faculty of Geology, Universitat de Barcelona, C/ Martí Franquès s/n, 08028 Barcelona, Spain

[4]Institute of Earth Sciences Jaume Almera - CSIC, C/Lluís Solé i Sabarís s/n, 08028 Barcelona, Spain

[5]Instituto de Investigaciones Marinas – CSIC, Eduardo Cabello 6, 36208 Vigo, Spain

[6]Pyrenean Institute of Ecology - CSIC, Av. Montañana 1005, 50059 Zaragoza, Spain

***Correspondence to:**

Roberto Bao

Centro de Investigacións Científicas Avanzadas (CICA), Facultade de Ciencias, Universidade da Coruña, 15701 A Coruña, Spain

Phone: +34 881 012 101

Fax: +34 981 16 70 65

E-mail: roberto.bao@udc.es

ABSTRACT

The coupling of lake dynamics with catchment biogeochemistry is considered the key element controlling primary production in mountain lakes at time scales of a few decades to millennia, yet little is known on the impacts of the morphometry of lakes throughout their ontogeny. As Lake Chungará (Central Andean Altiplano, northern Chile) experienced long-term lake-level fluctuations that strongly modified its area:volume ratio, it is an ideal system for exploring the relative roles that long-term climatic shifts and lake morphometry play on biosiliceous lacustrine productivity. In this paper, we review previous data on the percent contents of total organic carbon, total inorganic carbon, total nitrogen, total biogenic silica, isotopic composition of organic matter, carbonates, and diatom frustules, as well as data on the abundance of the chlorophycean *Botryococcus braunii* in this lake for the period 12,400-1,300 cal yr BP. We also include new data on organic carbon and biogenic silica mass accumulation rates and the diatom assemblage composition of an offshore core dated using ^{14}C and U/Th.

Biosiliceous productivity in Lake Chungará was influenced by shifts in allochthonous nutrient inputs related to variability in precipitation. Humid phases dated at approx. 12,400 to 10,000 and 9,600 to 7,400 cal yr BP coincide with periods of elevated productivity, whereas decreases in productivity were recorded during arid phases dated at approx. 10,000 to 9,600 and 7,400 to 3,550 cal yr BP (Andean mid-Holocene Aridity Period). However, morphometry-related in-lake controls led to a lack of a linear response of productivity to precipitation variability. During the late Glacial to early Holocene, lowstands facilitated complete water column mixing, prompting episodic massive blooms of a large centric diatom, *Cyclostephanos* cf. *andinus*. Thus, moderate productivity could be maintained, regardless of aridity, by this phenomenon of morphometric eutrophy during the early history of the lake. The subsequent net increase in lake level introduced modifications in the area of the epilimnion sediments versus the total volume of the epilimnion, preventing complete overturn. Surpassing a certain depth threshold at approx. 8,300 cal yr BP caused cessation of the morphometric eutrophy conditions associated with *Cyclostephanos* cf. *andinus* superblooms. After 7,300 cal yr BP, the lake experienced a decrease in biosiliceous productivity and a change of state that involved a stronger dependence on

precipitation variability, with a lesser contribution of diatoms to the total primary productivity. Our results show that the interpretation of lacustrine paleoproductivity records as paleoclimatic archives needs to take into account the effects of changes in the epilimnion sediment area to epilimnion volume ratio in association with lake ontogeny.

Keywords: lake paleoproductivity, lake ontogeny, laminated sediments, diatoms, Andean Altiplano, Holocene

64 **1. INTRODUCTION**

65 Photosynthetic activity in periodically stratified lakes is generally restricted by phosphorous and
66 nitrogen concentrations in the epilimnion because the waters underneath, although richer in these
67 limiting nutrients, do not receive sufficient light to sustain significant primary productivity (Sterner,
68 2008). This vertical segregation is usually eliminated when deep mixing of the water column transports
69 bottom nutrient-rich waters upward to the euphotic zone. Nutrient and mixing gradients are, therefore,
70 primary drivers of phytoplankton dynamics and productivity in aquatic ecosystems (Winder & Hunter,
71 2008). The morphometric characteristics of the lake basin influence the total epilimnion volume and
72 the degree of water column mixing and, thus, can be an important influence on lake productivity
73 (Imboden & Wüest, 1995; Wetzel, 2001).

74 The relative role that lake morphology plays in affecting productivity likely varies geographically and
75 over time. In a classical paper, Rawson (1955) reviewed data from a series of large lakes and
76 concluded that lake morphometry is a determinant factor in lacustrine productivity; this result,
77 however, could not be reproduced by Brylinsky & Mann (1973), who considered morphometry as
78 having relatively little impact on phytoplankton production. These ecological studies relied on space-
79 for-time substitution approaches (Smol, 2008) and did not consider changes in productivity that could
80 be associated with modifications in the morphology of an individual lake over long periods of time.
81 Moreover, despite evidence generated by Quaternary paleoecologists (Engstrom et al., 2000), many
82 limnologists still assume a traditional model of progressive lake eutrophication over time (Deevey,
83 1955). Indeed, temporal change in phytoplankton communities and their function is a time scale-
84 dependent process, the study of which has largely ignored the long-term variability resulting from lake
85 ontogeny (Anderson, 1995). Data analyses on broad time scales provide new insight into the role that
86 both climate and local physiographic factors have in affecting the productivity of lake systems, and
87 disentangling the relative importance of these two factors is required in Quaternary paleoclimatic
88 reconstructions that rely in part on the study of changes in paleoproductivity inferred from biosiliceous
89 proxy data (e.g., Johnson et al., 2004; Mackay, 2007; Castañeda et al., 2009).

Lakes in the Central Andean Altiplano experienced strong lake-level fluctuations during the Late Quaternary that altered their surface area:volume ratios (Placzek et al., 2009). This variation makes these lakes ideal systems for exploring not only the effects of long-term climatic shifts on primary productivity but also the way in which the lake morphometry dictates how lake-level fluctuations influence productivity. The millennial-scale moisture balance of the Atlantic-Amazon-hydrologic system is strongly influenced by precessional changes in solar insolation (e.g., Rowe et al., 2002) and tropical Atlantic sea-surface temperature (SST) variation (Baker et al., 2001). Changes in the Equatorial Pacific SST and El Niño-Southern oscillation (ENSO) variability may also have played a role (Polissar et al., 2013). All of these factors contributed to changes in lake levels that, in turn, affected the composition of planktonic communities (e.g., Tapia et al., 2003). Regardless, very little is known about the effects of long-term lake-level variability on the functional properties, such as lacustrine productivity, of regional limnological systems.

Lake Chungará (Central Andean Altiplano, northern Chile) is a surficially closed lake that has undergone significant changes in water level during the last 12,400 years (Sáez et al., 2007). Due to its complex bottom topography, these changes produced important modifications in the surface:volume ratio during its ontogeny, making it a good system to test the relative importance that climate and lake morphometric characteristics have on primary productivity variation. There is appreciable knowledge based on multiproxy evidence of the major changes that occurred in the lake since the Late Glacial, including sedimentary facies characterization (Sáez et al., 2007) and the isotopic composition of bulk organic matter ($\delta^{13}C_{org}$, $\delta^{15}N_{org}$; Pueyo et al., 2011), carbonates ($\delta^{18}O_{carbonate}$, $\delta^{13}C_{carbonate}$; Pueyo et al., 2011), and diatom frustules ($\delta^{18}O_{diat}$, $\delta^{13}C_{diat}$; Hernández et al., 2008, 2010, 2011, 2013). A moisture balance reconstruction based on magnetic susceptibility, X-ray fluorescence (XRF), X-ray diffraction (XRD), total carbon and total organic carbon (TC and TOC), biogenic silica (BSi) and a grey-color curve of the sediment data (Giralt et al., 2008) has also been published. Despite the large number of proxies analyzed, an overall picture of the causes underlying paleoproductivity changes in the lake is still lacking.

In this paper, we integrate previous and new (diatom assemblage composition, organic carbon and biogenic silica mass accumulation rates) multiproxy data on the paleoenvironmental evolution of Lake

Chungará to develop an evolutionary model of long-term productivity trajectories in a high-elevation tropical lake. We also study the relationship between changes in productivity and the main climatic events recorded in the Central Andean Altiplano as well as the potential role that lake morphometry could have played. We show how the imprinting of primary climatic forcing signals in the sedimentary record is decisively modulated by the effects of changes in the ratio of the area of the epilimnion sediments with respect to the total volume of the epilimnion throughout the ontogeny of the lake.

2. STUDY SITE

2.1 *Physiographic and limnological features*

Lake Chungará (18º15' S, 69º09' W, 4,520 m a.s.l., Fig. 1) was formed in the Paleo-Lauca River valley between 15,000 and 17,000 yr BP after the partial collapse of the Parinacota volcano, which originated at its earliest stages a very permeable barrier of breccia deposits dominated by large block-size particles (Clavero et al., 2002; Hora et al. 2007). The lake has a maximum length of 8.75 km, a maximum water depth of 40 m, a surface area of 21.5 km^2, and a volume of 400 x 10^6 m^3 (Mühlhauser et al., 1995; Herrera et al., 2006). The western and northern lake margins are steep, whereas the eastern and southern margins are gentle, forming extensive shallow (less than 7 m deep) platforms (Fig. 1B). The main inlet to the lake is the small Chungará stream (300-460 l s^{-1}), and the main route of water loss is via evaporation (3.10^7 m^3 yr^{-1}). Groundwater outflow to the nearby Cotacotani lakes has been estimated as approximately 6-7 10^6 m^3 yr^{-1} (Risacher et al., 1999; Dorador et al., 2003).

Lake Chungará is a cold-polymictic and moderately saline lake, which thermally stratifies from January to April (Mühlhauser et al., 1995). It contains 1.2 g l^{-1} of total dissolved salts, with a conductivity ranging between 1,500 and 3,000 μS cm^{-1}, and a water chemistry of the Na-Mg-HCO_3-SO_4 type (Mühlhauser et al., 1995; Dorador et al. 2003). The lake has been classified as oligo-mesotrophic or meso-eutrophic according to its chlorophyll-*a* concentration and photosynthetic activity, respectively (Mühlhauser et al., 1995). Most of the primary productivity is performed by diatoms, but cyanobacteria and chlorophyceans also contribute importantly during spring and summer

144 (Dorador et al., 2003; Márquez-García et al., 2009). Large concentrations of phosphorous were
145 recorded (Mühlhauser et al., 1995), but the lake is limited by nitrogen (Dorador et al., 2003; Márquez-
146 García et al., 2009). Maximum chlorophyll-*a* concentrations have been recorded during autumn
147 (Dorador et al., 2003).

148 The lake receives precipitation from the Atlantic Ocean. Annual rainfall in the Chungará region is
149 approximately 350 mm yr^{-1} but does vary (100-750 mm yr^{-1}). The mean temperature is 4.2ºC. Humidity
150 in the region is advected from the Amazon Basin by the South American Summer Monsoon (SASM),
151 which is linked to the Intertropical Convergence Zone (ITCZ) (Zhou & Lau, 1998). The wet season
152 occurs during the austral summer months, when a weak easterly flow prevails over the Altiplano as a
153 consequence of the southward migration of the subtropical jet stream and the establishment of the
154 Bolivian High Pressure system (Baker et al. 2005; Garreaud et al. 2009; Polissar et al., 2013). In
155 addition, a significant fraction of the inter-annual changes in summer precipitation is currently related
156 to ENSO (Garreaud et al., 2003).

157 2.2 *Lake sedimentary infill*

158 A 3D depositional model based on seismic imagery and sedimentary facies analyses of 15
159 sediment cores identified a total of 6 sedimentary units composed of 7 offshore, 3 littoral-nearshore,
160 and 2 volcaniclastic facies (Sáez et al., 2007) (Fig. 1C). Sediments in the offshore, deepest central
161 plain are composed of laminated (Unit 1) and non-laminated diatomaceous oozes with interbedded
162 tephra layers (Unit 2). The diatomaceous laminated sediments of Unit 1 show rhythmites consisting of
163 triplets (4 to 24 yr) of white, light- and dark-green laminae (Hernández et al., 2008, 2011) (Fig. 2).
164 Green laminae comprise a mixture of the euplanktonic diatom *Cyclostephanos andinus* (always
165 smaller than 50 µm), diatoms of the *Discostella stelligera* complex, and a diverse mixture of
166 tychoplanktonic and benthic diatoms. White laminae show an almost monospecific composition of very
167 large valves of *Cyclostephanos andinus* (>50 µm) resulting from the deposition of massive short-term
168 blooms of this taxon. These superblooms have been interpreted as being triggered by strong influx of
169 nutrient-rich waters from the lake bottom to the photic zone or, less frequently, by nutrient inputs
170 associated with increased runoff (Hernández et al., 2011). The dark laminae are considered to

171 represent the background limnological conditions. The diatomaceous oozes of Unit 2 show no
172 lamination or indication of massive short-term blooms of large *Cyclostephanos andinus*.

173

174 **3. MATERIALS AND METHODS**

175 In November 2002, 15 sediment cores up to 8 m long were retrieved from the lake using a
176 Kullenberg corer. From the core lithostratigraphic correlation, a composite core spanning the entire
177 sedimentary infill of the offshore zone (minimum thickness of 10 m) was constructed. The
178 chronological framework of the sedimentary sequence of Lake Chungará was generated from 17 AMS
179 ^{14}C dates of bulk organic matter and aquatic plant macrofossils and by one $^{238}U/^{230}Th$ date from
180 carbonates. The present-day reservoir effect of the lake was estimated in 3,260 yr BP, but it has been
181 considered to vary over time with changes in the volume:surface ratio of the lake in association with
182 water-level fluctuations (Giralt et al., 2008). Because of this, different corrections were applied to
183 lithological Units 1 and 2. The environmental status during the deposition of Unit 2b is considered akin
184 to that at present, as is the maximum water depth; for this reason, a constant reservoir effect of 3,260
185 yr was subtracted from the radiocarbon dates of Unit 2. Because it would be highly speculative to
186 estimate variations in the reservoir effect during the deposition of Unit 1, ages were calculated for the
187 two extreme reservoir values (i.e., minimum of 0 and maximum of 3,260 yr), and the mid point
188 between both values was employed to construct the age model. Accordingly, uncertainties in the
189 model are greatly reduced for Unit 2 (see further details in Giralt et al., 2008).

190 Samples for analyses were collected every 5-10 cm from core CHUN11A (Fig. 1). The TC and total
191 inorganic carbon (TIC) contents were measured using a UIC model 5011 CO2 Coulometer, with TOC
192 determined by subtracting TIC from TC. Total nitrogen (TN) was determined using a Variomax C/N
193 following the Dumas method (Ma & Gutterson, 1970). BSi was extracted using the alkaline leaching
194 technique (Mortlock & Froelich, 1989), measuring the resulting extract with the molybdate blue
195 colorimetric method (Hansen & Grashoff, 1983) using an AutoAnalyser Technicon II. The TOC, TIC
196 and TBSi results are expressed as percent values of the sediment dry weight. For the calculation of
197 dry bulk densities, the samples were dried to remove free water. Fluxes of TOC and BSi into the

198 sediments were estimated as mass accumulation rates (MARs, mg cm^{-2} yr^{-1}) by multiplying their
199 concentrations by the sediment dry densities and sedimentation rates at each depth. By calculating
200 the fluxes, the input of each component is independent of the effects of sediment dilution (Boyle,
201 2001). Although neither percent values nor MARs alone can provide precise paleoproductivity
202 reconstructions, their combined use can help in the identification of the main trends in productivity
203 (Engstrom & Wright, 1984; Boyle, 2001).

204 Samples for diatom analysis were processed using standard techniques (Renberg, 1990). At least
205 400 valves were counted per sampled interval. All counts were performed at X1000 using Nomarski
206 differential interference contrast optics. Diatom preservation was estimated by the *F* index (Flower &
207 Likhoshway, 1993), and identifications of diatom taxa were based upon the available diatom floras
208 from the region (Rumrich et al., 2000) and elsewhere (e.g., Krammer & Lange-Bertalot, 1986-1991;
209 Lange-Bertalot, 2000-2005). Raw valve counts were converted to percentage abundance data. All
210 statistical analyses were carried out on a diatom relative abundance matrix of those taxa attaining a
211 frequency of more than 2% in at least one sample. Data were transformed by square-root
212 transformation. Definition of the main Diatom Assemblage Zones (DAZs) was performed using
213 stratigraphically constrained cluster analysis based on squared Euclidean dissimilarity (CONISS,
214 Grimm, 1987), as implemented in Psimpoll 4.10 (Bennett, 2002). Zonations with variances that
215 exceeded the values generated by a broken-stick model of the distribution of variance were
216 considered to be statistically significant (Bennett, 1996).

217 Ordination analyses (Detrended Correspondence Analysis-DCA, and Principal Component
218 Analysis-PCA) were performed with the CANOCO 4.5 computer program (ter Braak & Šmilauer, 1998)
219 to identify the main underlying environmental gradients explaining the variability in the diatom
220 abundance data (Jongman et al., 1987). Although a transfer function for ionic concentration and
221 salinity was developed in the nearby Bolivian Altiplano (Sylvestre et al., 2001), most of the taxa
222 present in Lake Chungará do not occur in that dataset, and it was thus not useful for quantitative
223 paleoenvironmental reconstruction. Therefore, only qualitative diatom-based paleoenvironmental
224 reconstructions were performed, carefully informed by contemporary data on diatom ecology
225 (following Sayer et al., 2010). In this case, the qualitative approach was implemented on the basis of

226 the study of modern analogs in Lake Chungará (Dorador et al., 2003) and nearby Lake Titicaca
227 (Theriot et al., 1985; Iltis, 1992; Servant-Vildary, 1992; Tapia et al., 2003, 2004). Diatom autoecologies
228 derived from a survey of the literature (e.g., Servant-Vildary & Roux, 1990; Gasse et al., 1995;
229 Sylvestre et al., 2001) have also been used.

230 A tentative qualitative lake-level curve was constructed combining previous and new multiproxy
231 data, including the following: i) the abundance of euplanktonic vs. periphytic diatoms; ii) changes in
232 lithofacies, particularly the presence of carbonates (Sáez et al., 2007); iii) oxygen isotopic data on
233 diatom frustules ($\delta^{18}O_{diat}$) for the late Glacial and early Holocene, with $\delta^{18}O_{diat}$ enrichments and
234 depletions mostly indicating low and high lake levels, respectively (Hernández et al., 2013); iv) the
235 oxygen isotopic characterization of carbonates ($\delta^{18}O_{carbonate}$) starting to precipitate at 10,200 cal yr BP,
236 with $\delta^{18}O_{carbonate}$ depletions and enrichments indicating water volume increases and more evaporated
237 waters, respectively (Pueyo et al., 2011); v) the abundance of *Myriophyllum* sp. and *Botryococcus*
238 *braunii* (Sáez et al., 2007); and vi) the moisture balance reconstruction of Giralt et al. (2008).

239

240 **4. RESULTS**

241 **4.1 Diatom Assemblages**

242 A total of 109 taxa were identified. The percent abundance data of 21 common diatoms are plotted
243 stratigraphically in Fig. 3. The diatom record is dominated by euplanktonic diatoms (mainly
244 *Cyclostephanos andinus* and diatoms of the *Discostella stelligera* complex), with subdominant
245 freshwater tychoplanktonic and benthic taxa (mainly *Staurosira construens* aff. *venter*, *Cocconeis*
246 *placentula* and *Nitzschia tropica*). The diatom dissolution index *F* shows moderately well-preserved
247 valves in Unit 1, whereas diatom dissolution effects were more prominent in Unit 2 (Fig. 3). The
248 broken-stick model of the distribution of variance allowed the definition of eight DAZs (Table 1 and Fig.
249 3).

250 Previous preliminary examinations of smear slides (Hernández et al., 2008, 2011) did not allow
251 precise determinations at the species level. In the present study, routine counts allowed taxonomic

252 differences to be identified in specimens of *Cyclostephanos andinus* from the laminated sediments.
253 The valves found in the green laminae could be ascribed to the published description of
254 *Cyclostephanos andinus* (Tapia et al., 2004), whereas the larger specimens preserved in the white
255 laminae showed striking differences under microscopy. Later SEM ultrastructural examination of the
256 valves confirmed the uncertain taxonomic identity of larger *Cyclostephanos andinus*, which in the
257 future may be assigned to a new closely related species (cf. Fritz et al., 2012) or, alternatively, may be
258 considered *Cyclostephanos andinus* of extreme morphology (Edward Theriot, pers. comm.). Because
259 its taxonomic affinity is not yet affirmed, this species is herein referred to as *Cyclostephanos* cf.
260 *andinus*.

261 DCA was performed to estimate the length of the dominant gradient in the diatom assemblages
262 and to evaluate whether the taxa in the core samples followed a unimodal or linear distribution
263 (Jongman et al., 1987). The results indicated that the longest gradient was 2.08 SD units, suggesting
264 a linear response (Lepš & Šmilauer, 2003). For this reason PCA was subsequently performed. During
265 the implementation of the PCA, we sought to restrict our analyses to the identification of the main
266 long-term environmental forcings on the diatom assemblage composition. However, the white and light
267 green laminae of Unit 1 (Facies A and B), composed of a quasi-monospecific assemblage of
268 *Cyclostephanos* cf. *andinus*, represented very short-term conditions (extraordinary diatom blooms),
269 thereby interrupting any long-term trend (Hernández et al., 2008, 2011). This taxon was not present in
270 banded and massive Unit 2 (Facies D, E and F). To elucidate the effects of both sources of variation,
271 we performed Partial PCA using the lithological units (laminated, i.e., Unit 1, vs. non-laminated, i. e,
272 Unit 2) as covariables (ter Braak & Šmilauer, 1998; Lepš & Šmilauer, 2003). This procedure allowed
273 us to ascertain whether any environmental explanation of the long-term changes in the diatom record
274 remained after the effects of the short-term variability imposed by the white laminae were removed.

275 The first two principal components of the partial PCA (PC1 and PC2) explained 83.6% of the total
276 variance (λ_1 = 0.625; 69.4%, and λ_2 = 0.128; 14.2%). *Cyclostephanos andinus* showed the highest
277 score for the first main direction of variation (PC1), with diatoms of the *Discostella stelligera* complex
278 exhibiting the most negative score (Fig. 4). The second ordination axis (PC2) showed the highest
279 scoring for *Cyclostephanos* cf. *andinus*, with most of the periphytic taxa (e.g., *Nitzschia tropica*,

Staurosira construens aff. *venter*, *Fragilaria capucina*) also showing positive scores. At the opposite side of the gradient, *Cyclostephanos andinus* showed the most negative score. Variations in the first two principal components throughout the core are plotted in the diatom abundance diagram shown in Fig. 3.

4.2 Geochemical proxy data

The depositional evolution of Lake Chungará was reconstructed based on sedimentary facies analyses and a number of geochemical proxies. The percent values and MARs of TOC and TBSi, percent content of TIC, and the TOC/TN atomic ratio are plotted along with the percent abundance of benthic diatoms, used here as a rough indicator of changes in water depth, and the scores of the first two axes derived from the PCA performed using diatom abundance data (Fig. 5). Additionally, previous isotopic data on organic matter, carbonates, and diatom frustules and the percent abundance of *Botryococcus braunii* observed in palynological slides (Sáez et al., 2007) are also included.

4.2.1 *Unit 1*

The TBSi content in Unit 1 is high, ranging from 41 to 54%. Fairly stable TBSi values occur from the bottom to 531 cm (approx. 9,350 cal yr BP), comprising Subunit 1a and the lower part of Subunit 1b. The fairly constant percent content of Subunit 1a and the lower part of Subunit 1b is, however, not mirrored by the TBSi MARs data, which show a rising trend from 6.6 mg TBSi cm^2 yr^{-1} to a maximum flux for the entire sedimentary record of 29.2 mg TBSi cm^2 yr^{-1} recorded in Subunit 1a at 652 cm (approx. 10,600 cal yr BP). This trend is followed by a decline to a minimum value of 5.4 mg TBSi cm^2 yr^{-1}, which, again, is not accompanied by significant variations in the percentage of TBSi. Maximum values for the percent content of TBSi are recorded in the top half of Subunit 1b, with a maximum of 75% at 474 cm (approx. 8,600 cal yr BP), declining thereafter. This rise is paralleled by an increase in the TBSi flux to sediments, reaching values as high as 19.2 mg TBSi cm^2 yr^{-1}.

Although TOC and TBSi MARs follow a similar pattern, other differences are highlighted, especially when %TOC is considered. The bottom of Subunit 1a shows a declining trend in %TOC, followed by

306 an overall persistent rising trend throughout Subunits 1a and 1b. This trend begins at 787 cm (approx.
307 11,600 cal yr BP), when a minimum of 2.5% TOC is recorded, coinciding with the onset of the
308 Holocene. With regard to TOC (8.3%) and its accumulation rate (4.0 mg TOC cm^2 yr^{-1}), the highest
309 values in the entire unit correspond to the 682 cm level (approx. 10,950 cal yr BP), when a small
310 decrease in both the content of TBSi and its MAR is also recorded. The TOC flux to sediments
311 declines after this peak, until a minimum of 0.9 mg TOC cm^2 yr^{-1} at 550 cm (approx. 9,600 cal yr BP).
312 The %TOC value shows, however, a general increasing trend that fluctuates between 4.7 to 8.6%.

313 This unit ends at 450 cm (approx. 8,300 cal yr BP) with a strong reduction in the flux of TBSi and
314 TOC to sediments, as well as with the reduction in their percent content, which is concomitant with the
315 first occurrence of carbonate-rich layers and a sharp increase in %TIC (3.8%). Although a previous
316 TIC peak occurred at 550 cm (approx. 9,500 cal yr BP), it was not associated with discrete carbonate
317 laminae.

318 The atomic TOC/TN ratio shifts between 6.9 and 12.6 throughout this unit (a large decline at 712
319 cm, approx. 11,000 cal yr BP, can certainly be attributed to an analytical error), and although a rising
320 trend is visible throughout Subunits 1a to 1b, most of the values fall within the <10 range.

321 4.2.2 *Unit 2*

322 Flux values of 24.4 mg TBSi cm^2 yr^{-1} and 3.6 mg TOC cm^2 yr^{-1} begin to appear in Unit 2. After the
323 %TIC peak that separates Unit 1 from Unit 2, %TBSi rises to a maximum of 62.8 for the entire unit at
324 422 cm (c. 8,000 cal yr BP), whereas %TOC also increases to 9.2 at the same level. Immediately
325 thereafter, there is a declining trend from this level, involving a sharp fall in the case of TBSi after 337
326 cm (approx. 7,200 cal yr BP). TBSi MARs and %TBSi reach the lowest values for the entire record
327 from this time to present, with values that range between 1.8 to 8.8 mg TBSi cm^2 yr^{-1} and 6.3 to
328 34.8%, respectively. TOC fluxes are also strongly reduced, ranging from 0.4 to 2.5 mg TOC cm^2 yr^{-1},
329 but maintaining values above those of the Late Glacial. In contrast, %TOC shows substantial
330 fluctuations, with a peak at 22 cm (approx. 1,500 cal yr BP) of 9.7%. Reductions in TOC and TBSi
331 contents are, however, magnified by the presence of tephra layers at 224, 56 and 39 cm. In spite of
332 the general decrease in the geochemical paleoproductivity proxies, a consistent rising trend is

observed between 308-255 cm (approx. 6,900-6,400 cal yr BP), when %TBSi and %TOC show a parallel increase coincident with a maximum value of 4.4 for TIC.

The TOC/TN curve shows oscillations throughout the record, albeit maintaining a general increasing trend toward the present. This is most evident when the flux of TBSi is strongly reduced after 337 cm (approx. 7,200 cal yr BP). As is the case for %TBSi, %TOC and %TIC, there is also a consistent increase in the TOC/TN ratio between 308-255 cm (approx. 6,900-6,400 cal yr BP) when the highest values for the entire record (14.0 and 14.5) are reached.

5. DISCUSSION

5.1 Significance of the diatom assemblages

The diatom record of Lake Chungará is characterized by the shifting dominance of large vs. small taxa, typified by *Cyclostephanos andinus* and *Discostella stelligera*, respectively. These periods are interrupted by episodes of the exclusive dominance of a very large diatom, *Cyclostephanos* cf. *andinus*, manifested in the deposition of white, beige, and very light green laminae. Both *Cyclostephanos andinus* and diatoms of the *Discostella stelligera* complex represent high lake-level conditions without elevated salt concentrations (Tapia et al., 2003).

Cyclostephanos is a genus of euplanktonic diatoms characteristic of well-mixed waters under isothermal conditions (Håkansson, 2002), whereas diatoms of the *Discostella stelligera* complex thrive well in stratified low-energy environments (e.g., Rühland et al., 2008). Large cells, such as those of *Cyclostephanos andinus* and *Cyclostephanos* cf. *andinus*, require well-mixed conditions to avoid sinking in the water column (Margalef, 1978). In addition, large diatoms have increased nutrient requirements, and their low surface to volume area (S/V) reduces nutrient uptake. For these reasons, large diatoms only thrive well under high nutrient concentrations (Finkel et al., 2005; Litchman et al., 2009). Although there is no specific information on *Cyclostephanos andinus*, it can be hypothesized that the aforementioned requirements for large centric diatoms also apply to this and other closely related taxa. Conversely, the enhanced buoyancy of small-sized phytoplankton, such as components

359 of the *Discostella stelligera* complex, offers an advantage under thermal stratification, and the high S/V
360 ratio of these cells facilitates nutrient uptake under conditions of lower nutrients. Although factors other
361 that the water column mixing regime can simultaneously explain the abundance of centric diatoms in
362 sedimentary records (Saros & Anderson, 2014), comparison with modern analogs shows that
363 ecophysiological adaptations to avoid sinking are most likely the main driver of the abundance of
364 *Cyclostephanos* and *Discostella* in Lake Chungará. Diatoms of the *Discostella stelligera* group are
365 currently more abundant during austral summer, when stratification is favored (Dorador et al., 2003),
366 and this taxon is also most abundant in the nearshore regions of Lake Titicaca, where waters are
367 warmer (Tapia et al. 2003). In contrast, *Stephanodiscus astraea*, the former name for *Cyclostephanos*
368 *andinus* (Theriot et al., 1985; Tapia et al., 2004), was found to be the main component of the
369 phytoplankton assemblages in the cold season, when mixing due to isothermal conditions can be
370 promoted (Dorador et al., 2003). This result also fits with the known ecology of the species in Lake
371 Titicaca, in that it is associated with the breakdown of thermal stratification and relatively high levels of
372 nutrients, which range during maximum abundances of the taxon of approx. 1.5-4.5 μg-atoms l^{-1} of
373 NO_3-N, approx. 0.5-0.7 μg-atoms l^{-1} of soluble reactive P, and approx. 5-14 μg-atoms l^{-1} of SiO_2-Si
374 (Theriot et al., 1985). Iltis (1992) also reported blooms, when 100% of the diatom assemblage
375 comprises *Cyclostephanos andinus* (Servant-Vildary, 1992).

376 Results of PCA indicate that changes in the water column mixing regime and depth are the primary
377 controllers of the composition of diatom assemblages. As PC1 mainly reflects variations in the large
378 centric diatom *Cyclostephanos andinus* relative to small diatoms of the *Discostella stelligera* complex,
379 it measures the euplanktonic diatom size distribution, which is related to water turbulence (Fig. 5). The
380 high abundance of *Cyclostephanos andinus* throughout the history of the lake suggests that intervals
381 of isothermal mixing persisted. Nevertheless, their duration does appear to have varied in comparison
382 with stratification periods, as indicated by fluctuations in the relative abundance of the *Discostella*
383 *stelligera* group.

384 Changes in water depth are suggested by PC2 because it reflects variation in a set of periphytic
385 diatoms (e.g., *Nitzschia tropica*, *Staurosira construens* aff. *venter*, *Fragilaria capucina*.) vs.
386 euplanktonic *Cyclostephanos andinus* (Fig. 4). However, *Cyclostephanos* cf. *andinus* does show a

387 close relationship with periphytic taxa, which suggests that, although euplanktonic, it requires
388 moderately shallow waters to generate blooms. An association with shallow waters has also been
389 found for other species of the *Cyclostephanos andinus* complex that became extinct during the
390 Quaternary (Fritz et al., 2012). In Lake Titicaca, the largest-sized cells of the nominate
391 *Cyclostephanos andinus* were also found to be preferentially related to shallow environments
392 (Servant-Vildary, 1992). Additionally, the very large size of *Cyclostephanos* cf. *andinus* indicates not
393 only a well-mixed water column but also an enhanced nutrient storage capacity (Litchman et al.,
394 2009). Thus, *Cyclostephanos* cf. *andinus* superblooms, as well as the deposition of white laminae,
395 would be triggered by increased nutrient input during periods of shallow water. Although the
396 entrainment of littoral species in hyperpycnal flow into deeper waters during periods of extremely high
397 precipitation could be invoked to explain the mixture of periphytic and euplanktonic diatoms, no
398 significant changes in grain size were observed in the laminae bearing *Cyclostephanos* cf. *andinus*.
399 Moreover, a lamina-by-lamina isotopic diatom characterization showed that the deposition of white
400 laminae occurs mainly at times of increases in $\delta^{18}O_{diat}$ values, indicating reduced external hydrologic
401 inputs to the lake and depletions in $\delta^{13}C_{diat}$, an indicator of light carbon upwelled from the hypolimnion
402 to the epilimnion at this sampling scale (Hernández et al., 2011). All these data support the
403 interpretation of *Cyclostephanos* cf. *andinus* as a suitable indicator of conditions when nutrients stored
404 in the hypolimnion are released to the epilimnion during relative lowstands that favor the entrainment
405 of hypolimnetic waters into surface waters.

406

407 **5.2 Paleoecological evolution of Lake Chungará and relationship with major climatic events**

408 Sedimentological, micropaleontological, and geochemical indicators were used to define the
409 depositional evolution of Lake Chungará and a qualitative paleohydrological history characterized by
410 several low and highstand phases during the period 12,400-1,300 cal yr BP (Figs. 5 and 6). The
411 multiproxy approach followed in this review also allowed us to identify up to seven distinct productivity-
412 related stages in the paleoenvironmental evolution of the lake.

413

414 5.2.1 *Stage 1 (approx. 12,400–12,100 cal yr BP)*

415 Reduced productivity conditions are recorded at this initial stage, as indicated by the relatively low
416 fluxes of TOC and TBSi to sediments (Fig. 5). The highest abundance of benthic diatoms suggests
417 that depth conditions were among the lowest for the entire record (Fig. 6). A low lake level is also
418 supported by the presence of pollen belonging to the aquatic macrophyte *Myriophyllum* sp. and a very
419 low concentration of the chlorophycean *Botryococcus braunii* (Sáez et al., 2007). Values of PC1
420 suggest complete water column mixing to the bottom and nutrient release both coherent with a low
421 lake level. Interestingly, this period of low lake level in Chungará corresponds to a well documented
422 period of increased wetness in the Altiplano between 13,000 and 11,500 cal yr BP (Baker et al., 2001).
423 Furthermore, given the reconstructed shallow waters, probable cold conditions associated with the
424 Late Glacial could have potentially prevented high productivity. To reconcile a relatively shallow
425 depositional environment during a regional relatively wetter period, we have to take into account that
426 Lake Chungará was in the early stages of its evolution, after the partial collapse of the Parinacota
427 volcano dammed the paleo-Lauca River (Clavero et al., 2002). The age of the collapse is not well
428 constrained, but the most likely estimate ranges 15,000 – 17,000 cal yr BP, with the oldest sediments
429 deposited in the lake basin sometime between 15,500 and 12,800 cal yr BP (Sáez et al., 2007). Both
430 seismic data and multicore correlation (Sáez et al., 2007) are coherent with this timing for the origin of
431 the lake. During this interval, relatively low lake level depositional environments dominated the
432 Chungará Basin, indicating a more negative water balance, in spite of higher water input during a
433 regional wet period (Baker et al., 2001). This apparent contradiction could be solved considering that
434 large groundwater losses through the very permeable volcanic breccia barrier would occur during the
435 early stages of lake development. Only when fine lacustrine deposits progressively sealed the lake
436 basin, groundwater losses decreased and the lake level could rapidly increase (Hernández et al.,
437 2008).

438 So, relatively low lake levels prior to 12,100 cal yr BP in Lake Chungará do not reflect a low
439 precipitation phase and they are explained by the unique hydrogeological features of the newly-formed
440 lake. Moreover, the wet conditions at c. 12,000 cal yr BP in the Altiplano (Baker et al., 2001) would
441 have helped the rapid water infilling of Lake Chungará after its formation.

442 5.2.2 *Stage 2 (approx. 12,100–10,800 cal yr BP)*

443 This stage shows a significant reduction in benthic diatoms, which, however, still maintain high
444 values, indicating that shallow waters persisted. A progressive increase in %TOC starting at approx.
445 11,400 cal yr BP, as well as the highest MARs values for TBSi and TOC, indicate a period of
446 enhanced productivity (Fig. 5), an interpretation also supported by the observed $\delta^{13}C_{diat}$ and $\delta^{15}N_{org}$
447 enrichments (Pueyo et al., 2011; Hernández et al., 2013) (Fig. 5). This increase is concomitant with
448 highstand P1 and could be explained by a mechanism of nutrient inputs into the lake by runoff
449 (Dorador et al., 2003).

450 The *Discostella stelligera* complex dominated the first part of this stage (DAZ CHUN11A-02, Fig.
451 3), suggesting a stratified water column (Fig. 6). Relatively shallow waters during the first part of this
452 interval were, however, also favorable for the development of *Cyclostephanos* cf. *andinus*
453 superblooms, leading to the intermittent formation of white laminae (Facies A). The dominant stratified
454 conditions were, therefore, disturbed by sporadic and short-term episodes of strong turbulence. As the
455 change in the PC1 shows, the second part of this stage (most of DAZ CHUN11A-03) was
456 characterized by long periods of a well-mixed water column and high nutrient levels in surface waters,
457 concomitant with a peak in productivity conditions, as indicated by TOC and TBSi MARs (Fig. 5). The
458 change in the mixing regime is also reflected in the depletion of $\delta^{13}C_{org}$, which occurred between the
459 two parts of this period (Pueyo et al., 2011) and is likely related to enrichment of the epilimnion with
460 light carbon under periods of enhanced mixing (Meyers, 1997; Cohen, 2003). The fact that the
461 magnitude of $\delta^{13}C_{diat}$ enrichment does not keep pace with the increase in TOC and TBSi MARs was
462 also interpreted as an evidence of the intensification of mixing because this would have released
463 isotopically depleted CO_2 from the hypolimnion, buffering the $\delta^{13}C_{diat}$ increase due to enhanced
464 productivity. However, intermittent peaks in *Botryococcus braunii*, an indicator of increased water
465 column stability (Margalef, 1983), suggest a marked seasonality in the mixing regime.

466 The lake level remained relatively shallow during this period, even though a progressive rise is
467 suggested by the relative decrease in benthic diatoms. Nonetheless, the paleohydrological change
468 appears smaller than in areas further north, where wet conditions occurred in Lake Titicaca between

469 approx. 13,000 to 11,000 cal yr BP (Baker et al., 2001; Tapia et al., 2003), correlating with the wet
470 Coipasa lake cycle in most of the Bolivian Alitplano (Servant et al., 1995).

471 5.2.3 *Stage 3 (approx. 10,800–10,000 cal yr BP)*

472 This stage is characterized by a decrease in benthic diatoms after a significant peak at the onset of
473 this phase. Interestingly, the $\delta^{18}O_{diat}$ record during this interval shows an enrichment that is
474 contradictory to a highstand situation (Hernández et al., 2008) (Fig. 5). The results suggested that
475 flooding of the shallow eastern and southern platforms (Fig. 1B) at this time increased the entire S/V
476 ratio of the lake and, therefore, evaporation, explaining the $\delta^{18}O_{diat}$ enrichment. In this scenario, the
477 peak in benthic diatoms at the start of this stage could be a consequence of the topographic effect of
478 the increased availability of shallow littoral habitats when flooding occurred rather than a product of a
479 decrease in the lake level (Stone & Fritz, 2004; Wigdhal et al., 2014).

480 Flooding of the shallow platform is paralleled by two significant changes: on the one hand, the
481 productivity apparently decreased, as shown by the reduction in the TOC and TBSi MARs (Fig. 5); on
482 the other, the mixing status changed from well mixed, represented by the later dominance of
483 *Cyclostephanos andinus*, to stratified conditions, represented by the dominance of the *Discostella*
484 *stelligera* group. In between this change, *Cyclostephanos* cf. *andinus* superblooms develop and trigger
485 white laminae deposition as a consequence of easier nutrient recycling in the new extensive shallow
486 areas of the lake.

487 Whereas the TOC flux declines, %TOC shows an increase during this stage (Fig. 5). The
488 postulated reduced mixing of the water column could have maintained low or anoxic conditions at the
489 lake bottom, as also suggested the $\delta^{13}C_{carbonate}$ values of approximately 7‰ (Pueyo et al., 2011) (Fig.
490 5). This would increase organic matter preservation and, therefore, %TOC values. This organic matter
491 is predominantly of phytoplanktonic origin, as indicated by the TOC/TN values of approximately 10
492 (Meyers, 1997, 2003). The increase in %TOC, while %TBSi is maintained at similar levels, indicates a
493 greater contribution of the non-diatom component of the original phytoplanktonic community. This
494 replacement of diatoms, most likely by motile phytoplankton, is what is expected with decaying
495 turbulence (Margalef, 1978).

496 5.2.4 *Stage 4 (approx. 10,000–9,600 cal yr BP)*

497 The highest relative abundance of benthic diatoms occurs in Holocene times during this stage,
498 suggesting a short-lived lowstand situation (Fig. 6). The lake levels would be again similar to those of
499 the first part of stage 3, which maximized the extension of shallow habitats. The rise in the TOC/TN
500 ratio suggests an increased contribution of the non-algal component, likely littoral macrophytes, to the
501 organic matter flux to the sediments. The peak in the abundance of mesosaline *Nitzschia tropica* might
502 indicate a saline concentration associated with a decline in the lake level (e.g., Bao et al., 1999), a
503 common feature at present, when precipitation is reduced (Dorador et al., 2003). A carbonate peak
504 also occurs at this time. Intense photosynthetic activity during the superblooms of *Cyclostephanos* cf.
505 *andinus* is the most probable driver of carbonate precipitation via the removal of CO_2 (Pueyo et al.,
506 2011). However, the decline in TOC and TBSi MARs suggests that although primary productivity was
507 extraordinarily high during the short-lived superblooms of *Cyclostephanos* cf. *andinus*, these had no
508 major effect on the long-term total biomass production, which decreased during this stage.

509 During this event, a significant change towards a more turbulent regime occurred (Fig. 6). This part
510 of the sedimentary record exhibits the highest values of Mn, as recorded by XRF analyses (Moreno et
511 al., 2007). Mn precipitation usually indicates the oxygenation of a previously anoxic hypolimnion
512 (Cohen, 2003), suggesting that the well-stratified conditions during the previous stage 3 would have
513 produced seasonal or persistent anoxia, which promotes increased Mn concentration in the water
514 column.

515 The short-lived lowstand that characterizes this stage points to a dry event in the region. Additional
516 data on $\delta^{18}O_{diat}$ (Hernández et al., 2013), the development of brown-white interbedding and carbonate-
517 bearing laminated diatomite facies (Sáez et al., 2007), and high-resolution multiproxy geochemical
518 and mineralogical data (Giralt et al., 2008) support this interpretation. The recorded fall in water level
519 matches with the summer insolation minimum at 10,000 yr (Berger & Loutre, 1991), which would favor
520 a northward shift of the ITCZ, a reduction in the strength of the SASM, and, thus, a period of reduced
521 moisture (Garreaud et al., 2009). This short-lived dry period might be related to a similar event
522 detected in Lake Titicaca at approximately 11,000 to 10,000 cal yr BP (Baker et al., 2001; Tapia et al.,

2003). Uncertainties associated with the age models constructed for lacustrine sequences in the central Andean Altiplano (Quade et al., 2008) and different climatic responses due to latitudinal effects (Abbott et al., 2003) might account for the observed differences in timing between the two records. The Lake Pacucha sedimentary record from the Peruvian Andes (Hillyer et al., 2009) shows a lowstand that peaked at approx. 10,000 cal yr BP, closely fitting the shallow water conditions in Lake Chungará.

5.2.5 *Stage 5 (approx. 9,600–7,400 cal yr BP)*

This stage shows a significant rise in lake level (highstand P2) manifested by the very low percent values of benthic diatoms and $\delta^{18}O_{diat}$ depletion (Fig. 5). The record, however, shows a carbonate precipitation peak at 8,300 cal yr BP, which is most likely related to Ca availability after the prolonged leaching of volcanic rocks in the catchment increased the concentration of Ca in the lake waters (Pueyo et al., 2011). Productivity is high, with a peak in %TBSi and increases in %TOC as well as in TBSi and TOC MARs. These conditions are also associated with $\delta^{13}C_{org}$ and $\delta^{15}N_{org}$ record peaks (Pueyo et al., 2011) and a net increase in $\delta^{13}C_{diat}$, another indicator of elevated productivity at this time (Hernández et al., 2013) (Fig. 5). The main factor responsible for high productivity may be enhanced nutrient inputs from the catchment associated with increased water availability (Giralt et al., 2008). During this stage, stratification most likely persisted for longer periods of time relative to isothermal mixing, as indicated by a decrease in PC1 and the beginning of the steady increase in *Botryoccocus braunii* (Fig. 5). This chlorophycean is currently the main component of the phytoplankton in Lake Chungará during the warmest summers, a time when intense stratification develops (Dorador et al., 2003). The high values of $\delta^{13}C_{org}$ also recorded at this time (Fig. 5) may be related to enhanced stratification that enriches DIC in ^{13}C as well as to increased productivity (Meyers, 1997; Cohen, 2003). Because of reduced mixing and a deeper water column, complete water column overturn would be hindered, preventing the nutrient release from the lake bottom that allows the maintenance of large centric diatoms. As a consequence of the restriction of the lake's internal nutrient cycling, *Cyclostephanos* cf. *andinus* superblooms cease, and a transition from laminated (facies B) to massive (facies C) sediments occurs.

550 This humid phase can be ascribed to a wet period spanning 10,000 to 8,000 cal yr BP, when Lake
551 Titicaca showed overflowing lake-level conditions (Baker et al., 2001; Tapia et al., 2003). The similar
552 duration of this period in Chungará and Titicaca and the similar time lag experienced by the previous
553 dry event suggest an association with the same phenomenon. Wetter conditions between 8,400-7,200
554 cal yr BP were also recorded in Lake Paco Cocha (Abbott et al., 2003), and shorter wet episodes that
555 also match in age with this Lake Chungará stage are known for Lake Pacucha (Hillyer et al., 2009) at
556 approx. 8,730 and 8,300 cal yr BP and Lake Potosí (Bolivia) at approx. 8,000 cal yr BP (Wolfe et al.,
557 2001).

558 5.2.6 *Stage 6 (approx. 7,400–3,550 cal yr BP)*

559 This stage begins with a sharp increase in benthic diatoms and an enrichment in $\delta^{18}O_{carbonate}$, both
560 indicating a reduction in water depth (lowstand P3). The flux of TOC and TBSi is strongly reduced,
561 even to levels below those of the Late Glacial for TBSi, and is not accompanied by a decrease in TOC
562 of the same magnitude (Fig. 5). The observation of a much greater reduction in TBSi than in TOC in
563 both percent content and MARs suggests that other organisms are replacing diatoms as primary
564 producers. *Botryococcus braunii* increases its abundance during this phase (Sáez et al., 2007), and
565 the TOC/TN ratio reaches the highest values for the entire record (Fig. 5). Both observations support
566 the idea that at least chloropyceans and macrophytes increased their contribution to total primary
567 productivity.

568 The diatom record shows a reduction in the *Discostella stelligera* group and sharp increase in
569 *Cyclostephanos andinus* during this phase, with both taxa codominating the assemblages (Fig. 3). A
570 less stable water column and lowstand conditions facilitating a more complete overturn favored
571 *Cyclostephanos andinus*. Nonetheless, the decrease in the lake water level never reached conditions
572 that allowed superblooms of *Cyclostephanos* cf. *andinus*. The codominance between the *Discostella*
573 *stelligera* group and *Cyclostephanos andinus* suggests that although water column-stability decreased
574 compared to the previous phase, thermal stratification was very common. This is also supported by
575 the high percentages of *Botryococcus braunii*.

This stage fits into the mid-Holocene aridity period in the Altiplano, roughly established between 9,000 to 4,000 cal yr BP, though the intensity and exact timing of this period varied over the region (Abbott et al., 2003). Maximum aridity conditions are recorded in Lake Titicaca between approx. 8,000 to 5,500 cal yr BP (Baker et al., 2001), a time range that resembles the dry phase in Lake Chungará from approx. 7,400 to 3,600 cal yr BP. Uncertainties in our age model are greatly reduced after 8,000 cal yr BP (Giralt et al., 2008), facilitating a correlation with the chronology of Lake Titicaca. The Lake Chungará record also demonstrates that the mid Holocene period was not homogeneous but rather consisted of fluctuating dry and wet conditions. According to the diatom record, the driest conditions would have developed between 7,400 and 6,600 cal yr BP, fitting with mineralogical and high-resolution XRF data (Giralt et al., 2008). In contrast, a wetter period occurred between approx. 6,600 to 6,000 cal yr BP, correlating with a wet episode from 7,500 (7,000) to 6,500 (6,000) cal yr BP also recorded in Lake Titicaca (Baker et al., 2001; Rowe et al., 2002; Tapia et al., 2003).

5.2.7 *Stage 7 (approx. 3,550–1,300 cal yr BP)*

This stage is represented by the record of Subunit 2b, for which volcanoclastic materials constitute a great part of the sediments (Sáez et al., 2007). Marked fluctuations in %TOC and its MAR can partially be an artifact due to the presence of tephras. There is, however, a consistent trend in the first part of this stage toward a general reduction in both the TOC content and fluxes, as well as in the TOC/TN ratio. This is coincident with a depletion in $\delta^{18}O_{carbonate}$, interpreted as the end of the previous arid phase (Pueyo et al., 2011). Because of this and the absence of any significant increase in the benthic diatom content, the changes reflected in the organic matter reaching the lake bottom at this time are likely due to the increased contribution of allochthonous organic matter associated with enhanced runoff. The reduction in *Cyclostephanos andinus* and increase in the *Discostella stelligera* group indicate a strengthening water column stratification, likely associated with higher lake levels (Fig. 6).

Sediment cores from lakes Titicaca, Lagunillas, and Umayo (Peru) show that this latest part of the Holocene corresponds to a highstand phase (Rowe et al., 2002; Ekdahl et al., 2008). The

603 establishment of over-flow conditions in lake Titicaca started after 4,000 to 3,100 cal yr BP (Baker et
604 al., 2001; Tapia et al., 2003), matching the onset of this paleoproductivity stage in Lake Chungará.
605 Different lowstands have, however, been identified during this phase in Lake Titicaca, indicating that
606 the period was far from stable (Abbott et al., 1997; Baker et al., 2005). Similar fluctuations in Lake
607 Chungará correspond to small peaks in benthic diatoms at approx. 2,800, 2,200 and 1,500 cal yr BP.
608 Relatively deeper waters at the coring site might have downweighted the magnitude of any changes
609 in benthic diatom abundance.

610

611 **5.3 Main drivers of long-term changes in biosiliceous productivity**

612 Paleoproductivity changes in Lake Chungará typically show good agreement with the main
613 paleoclimatic phases defined in the central Andean Altiplano based on a set of lacustrine records.
614 Indeed, climate has exerted a fundamental influence on changes in productivity, modifying
615 allochthonous nutrient inputs to the lake. The morphometry of the lake, however, dictates the influence
616 of lake-level variation on nutrient cycling, thereby modulating the magnitude of the climate imprint in
617 the sedimentary record.

618 5.3.1 *Nutrient availability associated with runoff*

619 Periods of enhanced productivity (Stages 2 and 5, Fig. 6) are coincident with periods of increased
620 runoff associated with elevated water availability in the Altiplano. Conversely, at times of aridity
621 (Stages 4 and 6, Fig. 6), the lake experienced reduced biomass production. This is in agreement with,
622 on the one hand, the enhanced nutrient delivery in this lake by runoff and, on the other, the present-
623 day pattern of phytoplanktonic biomass reduction that accompanies water level decreases in this lake
624 (Dorador et al., 2003). Our observations are consistent with the fact that the key element controlling
625 primary production in mountain lakes at time scales of a few decades to millennia is the coupling of
626 lake dynamics with the biogeochemistry of the catchment (Catalan et al., 2006).

627 5.3.2 *Effects of lake morphometry on internal nutrient recycling*

628 Nutrient availability depends not only on external inputs but also on internal recycling due to the
629 existing water column structure at a given time. Its change prompts shifts in phytoplankton
630 communities, which, in turn, affect primary productivity as well as higher trophic production (e.g.,
631 Margalef, 1978; Winder & Hunter, 2008). Three stages of well-stratified waters dominated by small-
632 sized diatoms of the *Discostella stelligera* group are identified (Stages 3, 5 and 7, Fig. 6). Higher
633 turbulence and mixing is associated with four periods in which the large *Cyclostephanos* species are
634 more prominent (Stages 1, 2, 4 and 6, Fig. 6). The early phases in lake ontogeny (Stages 1 to 3, Fig.
635 6) show a clear correspondence between stronger mixing and elevated productivity, as shown by the
636 correspondence between PC1 and TBSi and TOC MARs. An exception is the Late Glacial (Stage 1,
637 Fig. 6) when, despite the dominance of isothermal conditions, productivity was low, likely due to cold
638 temperatures. The highest productivity conditions in the entire lake history were recorded when
639 increased turbulence is added to the effects of enhanced runoff (Stage 2, Fig. 6).

640 A major paleoecological transition occurs after Stage 3, when phases with nutrient recycling by
641 stronger turbulent conditions appear to be uncoupled from diatom productivity at the time scale of the
642 sediment record. This is shown by the existence of periods characterized by well-stratified waters with
643 high productivity (Stage 5, Fig. 6) and others with less stratified conditions but reduced production
644 (Stages 4 and 6, Fig. 6). In the absence of reliable paleoindicators of factors that affect water
645 turbulence, such as wind stress, surface heat flux or turbidity currents, a very probable explanation for
646 this decoupling is that changes in lake level alter the effects of mixing (Imboden & Wüest, 1995),
647 causing a change in productivity levels. Lake Chungará exhibits a complex bottom topography,
648 combining steep shorelines with extensive shallow platform areas (Fig. 1B). The water-level
649 fluctuations experienced during its history produced major changes in the relative extent of potential
650 deep mixing areas in the lake. During lowstands, complete or almost complete mixing of the water
651 column to the lake bottom is facilitated. When the ratio of the area of the epilimnion sediments with
652 respect to the total volume of the epilimnion is high, nutrient remineralization is rapid, enabling
653 nutrients to be recirculated into the epilimnion (Fee, 1979). During the early stages (Stages 1 to 3, Fig.
654 6), low water levels allow wind-driven turbulence to easily reach the nutrient-rich hypolimnion at times
655 of enhanced vertical mixing; temperature permitting, this promotes productivity. As the lake-level rises

during the early to the mid Holocene, complete vertical mixing becomes more restricted, and the effects of periods of strong turbulence on diatom productivity intensification are reduced.

The combined effect of water mixing and the epilimnion sediment area to epilimnion volume ratio on the internal nutrient supply is particularly well illustrated in the formation of *Cyclostephanos* cf. *andinus* superblooms and, therefore, in the deposition of white laminae in lithological Unit 1. White laminae are predominantly formed during lowstand periods or when littoral platforms of Lake Chungará are flooded, forming extensive shallow areas (Hernández et al., 2011). Under these circumstances, nutrient release from the lake bottom is facilitated, triggering massive *Cyclostephanos* cf. *andinus* blooms. The maximum deposition of white laminae is recorded during a particularly pronounced lowstand in Stage 4, after a long period of seasonal or persistent anoxia (Stage 3) affected the lake (Fig. 6). The development of an oxygen-depleted hypolimnion (Stage 3, Fig. 6) would enrich the bottom waters with phosphorous (Cohen, 2003), which is ultimately released into the surface waters in the following stage, triggering *Cyclostephanos* cf. *andinus* superblooms. This mechanism explains the deposition of almost pure diatom oozes at times of extended shallow conditions when, for this reason, the lake experiences a state of morphometric eutrophy *sensu* Rawson (1955). This ephemeral condition, which relies on nutrient recycling from deep waters, has no great effect on TBSi and TOC flux to the sediments in the long term (Fig. 5). Nonetheless, the importance of morphometric eutrophy should not be neglected when comparing to the recent parts of the record. Once a depth threshold is surpassed during the early to mid Holocene transition (corresponding to the change from the laminated deposits of Unit 1 to massive Unit 2), mixing down to the bottom becomes more difficult, and the formation of *Cyclostephanos* cf. *andinus* superblooms is hindered. Any ulterior lowstand, such as those recorded during the mid-Holocene arid period, would have never resulted in the lake level being below that depth threshold. Consequently, productivity can no longer solely rely on internal nutrient recycling, and biosiliceous productivity falls to minimum levels. Compared to lowstands associated with more juvenile stages in lake ontogeny, when morphometric eutrophy was still possible, the TBSi flux is strongly reduced to levels below Late Glacial times.

Surpassing the depth threshold likely not only precipitated the termination of *Cyclostephanos* cf. *andinus* superblooms but also likely produced the extinction of this taxon, which is not presently found

684 in other lake systems of the central Andean Altiplano. Undescribed new species of *Cyclostephanos*
685 that became extinct have also been detected in Pleistocene sediments of Lake Titicaca (Fritz et al.,
686 2012). In Lake Chungará, as is true for Lake Titicaca, some of the putative new morphospecies may
687 be favored by conditions associated with shallower waters than the nominate *Cyclostephanos*
688 *andinus*.

689 5.3.3 *Volcanism*

690 In addition to variations in runoff, volcanic ash deposition could have affected biosiliceous
691 productivity as an external forcing factor. Increased silica loads associated with ashfall during volcanic
692 events have been reported to trigger enhanced diatom productivity in some lake systems (e.g., Lotter
693 et al., 1995; Cruces et al., 2006). The most significant change in Holocene volcanism in the area was
694 the renewed activity of the Parinacota volcano after 7,500 cal yr BP (Giralt et al., 2008). However,
695 despite the increased availability of silica via tephra deposition during the sedimentation of Unit 2,
696 biosiliceous productivity was significantly lowered in Lake Chungará. Furthermore, no significant
697 changes occurred in diatom assemblages after the different periods of tephra deposition. The
698 relationship between tephra deposition and diatom productivity is most likely a time scale-dependent
699 process. Some evidence points to the short-term reorganization of diatom assemblages, as well as
700 changes in productivity, after volcanic disturbance, but these effects last for no more than 5 years
701 (Cruces et al., 2006). Other observations indicate that volcanic silica loads do not provide the
702 sustained stimulus necessary to enhance productivity and that long-term trends in lake evolution are
703 not fundamentally affected by tephra inputs (Telford et al., 2004). A more detailed sampling would,
704 therefore, be necessary to definitively confirm the short-term consequences of airborne tephras on the
705 productivity conditions of Lake Chungará.

706

707 **6. CONCLUSIONS**

708 The sedimentary record of Lake Chungará reveals a complex interplay between climatic and
709 lacustrine morphometric controls that influence paleoproductivity throughout its evolution. Precipitation

710 variability over the Andean Altiplano has been a decisive primary forcing factor of changes in
711 allochthonous nutrient inputs and paleoproductivity during the studied period. The magnitudes of
712 changes in climate-driven impacts on the aquatic system are, however, modulated by morphometry-
713 related in-lake controls that show a lack of a linear response of lacustrine productivity to changes in
714 precipitation and, therefore, to climatic variability.

715 Variations in the water-column mixing regime acted as a key driver in long-term productivity
716 conditions, compensating for losses produced at times of decreased nutrient availability associated
717 with runoff. This is particularly well exemplified during the early Holocene (10,800-9,600 cal yr BP),
718 which includes two distinct paleoproductivity stages. During the first stage, the lake showed a
719 prevailing low oxic or anoxic situation in its hypolimnion, as well as more stratified conditions that,
720 irrespective of intervals of enhanced precipitation in the Andean Altiplano, led to a significant decrease
721 in productivity. During more arid phases in the early Holocene, the trend toward decreased
722 productivity was maintained; however, a complete overturn facilitated by a lowstand situation helped to
723 sustain episodic moderate productivity conditions via nutrient recycling from sediments. When this
724 morphometric eutrophy occurred, most of the biomass was produced through episodic superblooms of
725 a very large diatom, *Cyclostephanos* cf. *andinus*, which is strictly dependent on the existence of deep
726 water circulation and relatively shallow waters.

727 The effects of mixing of the water column therefore strongly depend on changes in water-level
728 fluctuations. Lake Chungará experienced a net long-term lake-level increase since its origin up to
729 approx. 8,300 cal yr BP, a time when maximum depth conditions were reached. Because of the
730 complex topography of the basin, this lake-level increase substantially modified the area of the
731 epilimnion sediments with respect to the total volume of the epilimnion. Once the depth threshold was
732 surpassed, a deeper lake prevented complete mixing of the water column to the bottom, and the
733 episodic superblooms of *Cyclostephanos* cf. *andinus* were no longer possible. This made the lake
734 more dependent on allochthonous nutrient inputs and, therefore, on climate variability. As a result, the
735 Andean mid-Holocene Aridity Period, lasting in Lake Chungará from approx. 7,400 to 3,550 cal yr BP,
736 resulted in a sharp decrease in productivity which, at least for diatoms, descended to levels below
737 Late Glacial times. Crossing the depth threshold not only sharply decreased lake productivity but was

738 also accompanied by a reduction in the relative role of diatoms as primary producers. Subsequently,
739 biosiliceous productivity never reached the levels of previous stages in the lake ontogeny.

740 Our results for this closed high mountain lake show that climatic changes constitute a primary
741 driver in long-term productivity conditions but that the magnitude of change can be strongly amplified
742 or reduced by factors intrinsic to the lake that vary during its ontogeny. This needs to be taken into
743 account when interpreting lacustrine paleoproductivity records as evidence of late Quaternary climatic
744 changes.

745

746 **ACKNOWLEDGMENTS**

747 The Spanish Ministry of Science and Innovation funded this research through the projects
748 ANDESTER (BTE2001-3225), Complementary Action (BTE2001-5257-E), LAVOLTER (CGL2004-
749 00683/BTE), GEOBILA (CGL2007-60932/BTE) and CONSOLIDER-Ingenio 2010 GRACCIE
750 (CSD2007-00067). The Limnological Research Center (USA) provided the technology and expertise
751 to retrieve the cores. We are grateful to CONAF (Chile) for the facilities provided in Parque Nacional
752 Lauca. Special thanks are due to Sherilyn Fritz for her contributions over the years to help us
753 understand the paleoecology of Lake Chungará and to an anonymous reviewer for critical comments
754 and suggestions that greatly improved the manuscript. We are also indebted to Edward Theriot, who
755 examined scanning electron microscope micrographs of *Cyclostephanos* comprising the laminated
756 unit. Manel Leira is also thanked for his advice on statistical analyses.

757

758 **REFERENCES**

759
760 Abbott, M.B., Binford, M.W., Brenner, M., Kelts, K., 1997. A 3500 14C yr high-resolution record of
761 water-level changes in Lake Titicaca, Bolivia/Peru. Quaternary Research 47, 169-180.
762 Abbott, M.B., Wolfe, B.B., Wolfe, A.P., Seltzer, G.O., Aravena, R., Mark, B.G., Polissar, P.J., Rodbell,
763 D.T., Rowe, H.D., Vuille, M., 2003. Holocene paleohydrology and glacial history of the central
764 Andes using multiproxy sediment studies. Palaeogeography, Palaeoclimatology and
765 Palaeoecology 194, 123-138.
766 Anderson, N.J., 1995. Temporal scale, phytoplankton ecology and paleolimnology. Freshwater Biology

767 34, 367-378.
768 Baker, P.A., Fritz, S.C., Garland, J., Ekdahl, E., 2005. Holocene hydrologic variation at Lake Titicaca,
769 Bolivia/Peru, and its relationship to North Atlantic climate variation. Journal of Quaternary Science
770 20, 655-662.
771 Baker, P.A., Seltzer, G.O., Fritz, S.C., Dunbar, R.B., Grove, M.J., Tapia, P.M., Cross, S.L., Rowe,
772 H.D., Broda, J.P., 2001. The history of South American tropical precipitation for the past 25,000
773 years. Science 291, 640-643.
774 Bao, R., Sáez, A., Servant-Vildary, S., Cabrera, L., 1999. Lake-level and salinity reconstruction from
775 diatom analyses in Quillagua formation (late Neogene, Central Andean Forearc, northern Chile).
776 Palaeogeography, Palaeoclimatology, Palaeoecology 153, 309-335.
777 Bennett, K.D., 1996. Determination of the number of zones in a biostratigraphical sequence. New
778 Phytol. 132, 155-170.
779 Bennett, K.D., 2002. Documentation for Psimpoll 4.10 and Pscomb 1.03, C Programs for Plotting
780 Pollen Diagrams and Analising Pollen Data. Uppsala University.
781 Berger, A., Loutre, M.F., 1991. Insolation values for the climate of the last 10 million years. Quaternary
782 Science Reviews 10, 297-317.
783 Boyle, J.F., 2001. Inorganic geochemical methods in paleolimnology, In: Last, W.M., Smol, J.P. (Eds.),
784 Tracking Environmental Change Using Lake Sediments. Volume 2: Physical and Geochemical
785 Methods. Kluwer Academic Publishers, Dordrecht, pp. 83-141.
786 Brylinsky, M., Mann, K.H., 1973. An analysis of factors governing productivity in lakes and reservoirs.
787 Limnology and Oceanography 18, 1-14.
788 Castañeda, I.S., Werne, J.P., Johnson, T.C., 2009. Influence of climate change on algal community
789 structure and primary productivity of Lake Malawi (East Africa) from the Last Glacial Maximum to
790 present. Limnology and Oceanography 54, 2431-2447.
791 Catalan, J., Camarero, L., Felip, M., Pla, S., Ventura, M., Buchaca, T., Bartomeus, F., De Mendoza,
792 G., Miró, A., Casamayor, E.O., Medina-Sánchez, J.M., Bacardit, M., Altuna, M., Bartrons, M.,
793 Díaz de Quijano, D., 2006. High mountain lakes: extreme habitats and witnesses of
794 environmental changes. Limnetica 25, 551-583.
795 Clavero, J.E., Sparks, S.J., Huppert, H.E., 2002. Geological constraints on the emplacement
796 mechanism of the Parinacota debris avalanche, northern Chile. Bulletin of Volcanology 64, 40-54.
797 Cohen, A.S., 2003. Paleolimnology. Oxford University Press, Oxford.
798 Cruces, F., Urrutia, R., Parra, O., Araneda, A., Treutler, H., Bertrand, S., Fagel, N., Torres, L., Barra,
799 R., Chirinos, L., 2006. Changes in diatom assemblages in an Andean lake in response to a recent
800 volcanic event. Archiv Fur Hydrobiologie 165, 23-35.
801 Deevey, E.S., 1955. The obliteration of the hypolimnion. Memorie dell'Istituto Italiano di Idrobiologia,
802 Suppl 8, 9-38.
803 Dorador, C., Pardo, R., Vila, I., 2003. Variaciones temporales de parámetros físicos, químicos y
804 biológicos de un lago de altura: el caso del lago Chungará. Revista Chilena de Historia Natural
805 76, 15-22.
806 Ekdahl, E.J., Fritz, S.C., Baker, P.A., Rigsby, C.A., Coley, K., 2008. Holocene multidecadal- to
807 millennial-scale hydrologic variability on the South American Altiplano. The Holocene 18, 867-
808 876.
809 Engstrom, D.R., Fritz, S.C., Almendinger, J.E., Juggins, S., 2000. Chemical and biological trends
810 during lake evolution in recently deglaciated terrain. Nature 408, 161-166.
811 Engstrom, D.R., Wright Jr., H.E., 1984. Chemical stratigraphy of lake sediments as a record of
812 environmental change, In: Haworth, E.Y., Lund, J.W.G. (Eds.), Lake Sediments and
813 Environmental History. Leicester University Press, Leicester, pp. 11-68.
814 Fee, E.J., 1979. A relation between lake morphometry and primary productivity and its use in
815 interpreting whole-lake eutrophication experiments. Limnology and Oceanography 24, 401-416.
816 Finkel, Z.V., Katz, M.E., Wright, J.D., Schofield, O.M.E., Falkowski, P.G., 2005. Climatically driven
817 macroevolutionary patterns in the size of marine diatoms over the Cenozoic. Proceedings of the
818 National Academy of Sciences 102, 8927-8932.
819 Flower, R.J., Likoshway, Y., 1993. An investigation of diatom preservation in Lake Baikal, Fifth
820 Workshop on Diatom Algae, March 16-20, Irkutsk, Russia, pp. 77-78.
821 Fritz, S.C., Baker, P.A., Tapia, P., Spanbauer, T., Westover, K., 2012. Evolution of the Lake Titicaca
822 basin and its diatom flora over the last ~370,000 years. Palaeogeography, Palaeoclimatology,
823 Palaeoecology 317, 93-103.
824 Garreaud, R., Vuille, M., Clement, A.C., 2003. The climate of the Altiplano: observed current
825 conditions and mechanisms of past changes. Palaeogeography, Palaeoclimatology,
826 Palaeoecology 194, 5-22.

827 Garreaud, R.D., Vuille, M., Compagnucci, R., Marengo, J., 2009. Present-day South American climate.
828 Palaeogeography, Palaeoclimatology, Palaeoecology 281, 180-195.
829 Gasse, F., Juggins, S., Ben Khelifa, L., 1995. Diatom-based transfer functions for inferring past
830 hydrochemical characteristics of African lakes. Palaeogeography, Palaeoclimatology,
831 Palaeoecology 117, 31-54.
832 Giralt, S., Moreno, A., Bao, R., Sáez, A., Prego, R., Valero-Garcés, B., Pueyo, J., González-Sampériz,
833 P., Taberner, C., 2008. A statistical approach to disentangle environmental forcings in a
834 lacustrine record: the Lago Chungará case (Chilean Altiplano). Journal of Paleolimnology 40,
835 195-215.
836 Grimm, E.C., 1987. CONISS: a Fortran 77 program for stratigraphically constrained cluster analysis by
837 the method of incremental sum of squares. Computers and Geosciences 13, 13-35.
838 Håkansson, H., 2002. A compilation and evaluation of species in the general *Stephanodiscus*,
839 *Cyclostephanos* and *Cyclotella* with a new genus in the family Stephanodiscaceae. Diatom
840 Research 17, 1-139.
841 Hansen, H.P., Grashoff, K., 1983. Automated chemical analysis, In: Grashoff, M., Ehrhardt, M.,
842 Kremlin, K. (Eds.), Methods of Seawater Analysis. Verlag Chemie, Weinheim, pp. 368-376.
843 Hernández, A., Bao, R., Giralt, S., Barker, P.A., Leng, M.J., Sloane, H.J., Sáez, A., 2011.
844 Biogeochemical processes controlling oxygen and carbon isotopes of diatom silica in Late Glacial
845 to Holocene lacustrine rhythmites. Palaeogeography, Palaeoclimatology, Palaeoecology 299,
846 413-425.
847 Hernández, A., Bao, R., Giralt, S., Leng, M.J., Barker, P.A., Pueyo, J.J., Sáez, A., Moreno, A., Valero-
848 Garcés, B., Sloane, H.J., 2008. The palaeohydrological evolution of Lago Chungará (Andean
849 Altiplano, northern Chile) during the Lateglacial and early Holocene using oxygen isotopes in
850 diatom silica. Journal of Quaternary Science 23, 351-363.
851 Hernández, A., Bao, R., Giralt, S., Sáez, A., Leng, M.J., Barker, P.A., Kendrick, C.P., Sloane, H.J.,
852 2013. Climate, catchment runoff and limnological drivers of carbon and oxygen isotope
853 composition of diatom frustules from the central Andean Altiplano during the Lateglacial and Early
854 Holocene. Quaternary Science Reviews 66, 64-73.
855 Hernández, A., Giralt, S., Bao, R., Sáez, A., Leng, M., Barker, P., 2010. ENSO and solar activity
856 signals from oxygen isotopes in diatom silica during late glacial-Holocene transition in Central
857 Andes (18°S). Journal of Paleolimnology 44, 413-429.
858 Herrera, C., Pueyo, J.J., Sáez, A., Valero-Garcés, B.L., 2006. Relación de aguas superficiales y
859 subterráneas en el área del lago Chungará y lagunas de Cotacotani, norte de Chile: un estudio
860 isotópico. Revista Geológica de Chile 33, 299-325.
861 Hillyer, R., Valencia, B.G., Bush, M.B., Silman, M.R., Steinitz-Kannan, M., 2009. A 24,700-yr
862 paleolimnological history from the Peruvian Andes. Quaternary Research 71, 71-82.
863 Hora, J.M., Singer, B.S., Wörner, G., 2007. Volcano evolution and eruptive fl ux on the thick crust of
864 the Andean Central Volcanic Zone: $^{40}Ar/^{39}Ar$ constraints from Volcán Parinacota, Chile.
865 Geological Society of America Bulletin 119, 343-362.
866 Iltis, A., 1992. Phytoplankton. Quantitative aspects and populations, In: Dejoux, C., Iltis, A. (Eds.),
867 Lake Titicaca. A Synthesis of Limnological Knowledge. Kluwer Academic Publishers, Dordrecht,
868 pp. 182-195.
869 Imboden, D.M., Wüest, A., 1995. Mixing mechanisms in lakes, In: Lerman, A., Imboden, D.M., Gat,
870 J.R. (Eds.), Physics and Chemistry of Lakes. Springer-Verlag, Berlin, pp. 83-138.
871 Johnson, T.C., Brown, E.T., McManus, J., 2004. Diatom productivity in northern lake Malawi during the
872 past 25,000 years: implications for the position of the intertropical convergence zone at millenial
873 and shorter time scales, In: Battarbee, R.W., Gasse, F., Stickley, C.E. (Eds.), Past Climate
874 Variability through Europe and Africa. Springer, Dordrecht, pp. 932-116.
875 Jongman, R.H.G., ter Braak, C.J.F., van Tongeren, O.F.R., 1987. Data Analysis in Community and
876 Landscape Ecology. Pudoc, Wageningen, p. 299.
877 Krammer, K., Lange-Bertalot, H., 1986-1991. Bacillariophyceae, In: Ettl, H., Gerloff, J., Heynig, H.,
878 Mollenhauer, D. (Eds.), Süßwasserflora von Mitteleuropa. Fischer-Verlag, Stuttgart.
879 Lange-Bertalot, H., 2000-2005. Diatoms of the European Inland Waters and Comparable Habitats.
880 Volumes 1, 2, 3, 4, 5. A. R. G. Gantner Verlag, Ruggell, Liechtenstein.
881 Lepš, J., Šmilauer, P., 2003. Multivariate Analysis of Ecological Data using CANOCO. Cambridge
882 University Press, Cambridge.
883 Litchman, E., Klausmeier, C.A., Yoshiyama, K., 2009. Contrasting size evolution in marine and
884 freshwater diatoms. Proceedings of the National Academy of Sciences 106, 2665-2670.
885 Lotter, A.F., Birks, H.J.B., Zolitschka, B., 1995. Late-glacial pollen and diatom changes in response to
886 two different environmental perturbations: volcanic eruption and Younger Dryas cooling. Journal

887 of Paleolimnology 14, 23-47.
888 Ma, T.S., Gutterson, M., 1970. Organic elemental analysis. Analytical Chemistry 42, 105-114.
889 Mackay, A.W., 2007. The paleoclimatology of Lake Baikal: A diatom synthesis and prospectus. Earth-
890 Science Reviews 82, 181-215.
891 Margalef, R., 1978. Life forms of phytoplankton as survival alternatives in an unstable environment.
892 Oceanologica Acta 1, 493-509.
893 Margalef, R., 1983. Limnología. Ediciones Omega, Barcelona.
894 Márquez-García, M., Vila, I., Hinojosa, L.F., Méndez, M.A., Carvajal, J.L., Sabando, M.C., 2009.
895 Distribution and seasonal fluctuations in the aquatic biodiversity of the southern Altiplano.
896 Limnologica - Ecology and Management of Inland Waters 39, 314-318.
897 Meyers, P.A., 1997. Organic geochemical proxies of paleoceanographic, paleolimnologic, and
898 paleoclimatic processes. Organic Geochemistry 27, 213-250.
899 Meyers, P.A., 2003. Applications of organic geochemistry to paleolimnological reconstructions: a
900 summary of examples from the Laurentian Great Lakes. Organic Geochemistry 34, 261-289.
901 Moreno, A., Giralt, S., Valero-Garcés, B.L., Sáez, A., Bao, R., Prego, R., Pueyo, J.J., González-
902 Sampériz, P., Taberner, C., 2007. A 14 kyr record of the tropical Andes: The Lago Chungará
903 sequence (18°S, northern Chilean Altiplano). Quaternary International 161, 4-21.
904 Mortlock, R.A., Froelich, P.N., 1989. A simple method for the rapid determination of biogenic opal in
905 pelagic marine sediments. Deep-Sea Research 36, 1415-1426.
906 Mühlhauser, H.A., Hrepic, N., Mladinic, P., Montecino, V., Cabrera, S., 1995. Water quality and
907 limnological features of the Andean Lake Chungará, northern Chile. Revista Chilena de Historia
908 Natural 68, 341-349.
909 Placzek, C., Quade, J., Betancourt, J.L., Patchett, P.J., Rech, J.A., Latorre, C., Matmon, A., Holmgren,
910 C., English, N.B., 2009. Climate in the dry central Andes over geologic, millennial, and
911 interannual scales. Annals of the Missouri Botanical Garden 96, 386-397.
912 Polissar, P.J., Abbott, M.B., Wolfe, A.P., Vuille, M., Bezada, M., 2013. Synchronous interhemispheric
913 Holocene climate trends in the tropical Andes. Proceedings of the National Academy of Sciences
914 110, 14551-14556.
915 Pueyo, J.J., Sáez, A., Giralt, S., Valero-Garcés, B.L., Moreno, A., Bao, R., Schwalb, A., Herrera, C.,
916 Klosowska, B., Taberner, C., 2011. Carbonate and organic matter sedimentation and isotopic
917 signatures in Lake Chungará, Chilean altiplano, during the last 12.3 kyr. Palaeogeography,
918 Palaeoclimatology, Palaeoecology 307, 339-355.
919 Quade, J., Rech, J.A., Betancourt, J.L., Latorre, C., Quade, B., Rylander, K.A., Fisher, T., 2008.
920 Paleowetlands and regional climate change in the central Atacama Desert, northern Chile.
921 Quaternary Research 69, 343-360.
922 Rawson, D.S., 1955. Morphometry as a dominant factor in the productivity of large lakes.
923 Internationale Vereinigung fuer Theoretische und Angewandte Limnologie Verhandlungen 12,
924 164-175.
925 Renberg, I., 1990. A procedure for preparing large sets of diatom slides from sediment cores. Journal
926 of Paleolimnology 4, 87-90.
927 Risacher, F., Alonso, H., Salazar, C., 1999. Geoquímica de las aguas en las cuencas de cerradas: I, II
928 Regiones de Chile. Vol. II. Convenio de Cooperación DGA, UCN e IRD. Internal Report, p. 141.
929 Rowe, H.D., Dunbar, R.B., Mucciarone, D.A., Seltzer, G.O., Baker, P.A., Fritz, S., 2002. Insolation,
930 Moisture Balance and Climate Change on the South American Altiplano Since the Last Glacial
931 Maximum. Climatic Change 52, 175-199.
932 Rühland, K., Paterson, A.M., Smol, J.P., 2008. Hemispheric-scale patterns of climate-related shifts in
933 planktonic diatoms from North American and European lakes. Global Change Biology 14, 2740-
934 2754.
935 Rumrich, U., Lange-Bertalot, H., M., R., 2000. Diatomeen der Anden. Von Venezuela bis
936 Patagonien/Tierra del Fuego. A. R. G. Gantner Verlag K. G., Ruggell.
937 Sáez, A., Valero-Garcés, B.L., Moreno, A., Bao, R., Pueyo, J.J., González-Sampériz, P., Giralt, S.,
938 Taberner, C., Herrera, C., Gibert, R.O., 2007. Lacustrine sedimentation in active volcanic
939 settings: the Late Quaternary depositional evolution of Lake Chungará (northern Chile).
940 Sedimentology 54, 1191-1222.
941 Saros, J.E., Anderson, N.J., 2014. The ecology of the planktonic diatom *Cyclotella* and its implications
942 for global environmental change studies. Biological Reviews, http://doi.org/10.1111/brv.12120.
943 Sayer, C.D., Davidson, T.A., Jones, J.I., Langdon, P.G., 2010. Combining contemporary ecology and
944 palaeolimnology to understand shallow lake ecosystem change. Freshwater Biology 55, 487-499.
945 Servant, M., Fournier, M., Argollo, J., Servant-Vildary, S., Sylvestre, F., Wirrmann, D., Ybert, J.P.,
946 1995. La dernière transition glaciaire/interglaciaire des Andes tropicales sud (Bolivie) d'après

l'etude des variations des niveaux lacustres et des fluctuations glaciaires. Comptes Rendus Académie des Sciences Paris 320, 729-736.
Servant-Vildary, S., 1992. Phytoplankton. The diatoms, In: Dejoux, C., Iltis, A. (Eds.), Lake Titicaca. A Synthesis of Limnological Knowledge. Kluwer Academic Publishers, Dordrecht, pp. 163-175.
Servant-Vildary, S., Roux, M., 1990. Multivariate analysis of diatoms and water chemistry in Bolivian saline lakes. Hydrobiologia 197, 267-290.
Smol, J.P., 2008. Pollution of Lakes an Rivers. A Palaeoenvironmental Perspective. Blackwell Publishing, Malden.
Sterner, R.W., 2008. On the Phosphorus Limitation Paradigm for Lakes. International Review of Hydrobiology 93, 433-445.
Stone, J.R., Fritz, S.C., 2004. Three-dimensional modeling of lacustrine diatom habitat areas: Improving paleolimnological interpretation of planktic : benthic ratios. Limnology and Oceanography 49, 1540-1548.
Sylvestre, F., Servant-Vildary, S., Roux, M., 2001. Diatom-based ionic concentration and salinity models from the south Bolivian Altiplano (15–23°S). Journal of Paleolimnology 25, 279-295.
Tapia, P.M., Fritz, S.C., Baker, P., Seltzer, G.O., Dunbar, R., 2003. A Late Quaternary diatom record of tropical climatic history from Lake Titicaca (Peru and Bolivia). Palaeogeography, Palaeoclimatology, Palaeoecology 194, 139-164.
Tapia, P.M., Theriot, E., Fritz, S.C., Cruces, F., Rivera, P., 2004. Distribution and morphometric analysis of *Cyclostephanos andinus* comb. nov., a planktonic diatom from the Central Andes. Diatom Research 19, 311-327.
Telford, R.J., Barker, P., Metcalfe, S.E., Newton, A., 2004. Lacustrine responses to tephra deposition: examples from Mexico. Quaternary Science Reviews 23, 2337-2353.
ter Braak, C.J.F., Šmilauer, P., 1998. CANOCO reference manual and user's guide to CANOCO for Windows: Software for canonical community ordination (version 4). Microcomputer Power, Ithaca, New York.
Theriot, E., Carney, H.J., Richerson, P.J., 1985. Morphology, ecology and systematics of *Cyclotella andina* sp. nov. (Bacillariophyceae) from Lake Titicaca, Peru-Bolivia. Phycologia 24, 381-387.
Wetzel, R.G., 2001. Limnology. Academic Press, San Diego.
Wigdahl, C.R., Saros, J.E., Fritz, S.C., Stone, J.R., Engstrom, D.R., 2014. The influence of basin morphometry on the regional coherence of patterns of diatom-inferred salinity in lakes of the northern Great Plains (USA). The Holocene 24, 603-613.
Winder, M., Hunter, D., 2008. Temporal organization of phytoplankton communities linked to physical forcing. Oecologia 156, 179-192.
Wolfe, B.B., Aravena, R., Abbott, M.B., Seltzer, G.O., Gibson, J.J., 2001. Reconstruction of paleohydrology and paleohumidity from oxygen isotope records in the Bolivian Andes. Palaeogeography, Palaeoclimatology, Palaeoecology 176, 177-192.
Zhou, J., Lau, K.M., 1998. Does a Monsoon climate exist over South America? Journal of Climate 11, 1020-1040.

988 **TABLE CAPTION**

989 **Table 1.-** Summarized description of diatom assemblage zones (DAZs) from Lake Chungará

990

991

992

993 **FIGURE CAPTIONS**

994 **Figure 1.-** A. Location of sites cited in this paper. B. Catchment and main topographical features of
995 Lake Chungará. A star indicates the position of the studied core CHUN11A. The black line
996 corresponds to the cross-section (C) of the lake. C. Cross-section of the sediment infilling
997 of the lake. The position of the studied core is indicated by the sketch of the coring
998 platform. Lithological units are according to Sáez et al. (2007).

999 **Figure 2.-** A. Digital DMT CoreScan (LRC, Minnesota) image of laminated sediments of core
1000 CHUN11A. B. Micrograph (X100) of a petrographical thin-section showing a couplet
1001 composed of a green (bottom) and a white lamina (top). C. Detail (X400) showing the white
1002 lamina exclusively formed by skeletons of *Cyclostephanos* cf. *andinus*. D. *Idem* green
1003 lamina dominantly consisting of *Cyclostephanos andinus*, and some diatoms of the
1004 *Discostella stelligera* complex embedded in an organic matrix.

1005 **Figure 3.-** Diatom percentage diagram for selected taxa (≥2% abundance in at least one sample) of
1006 Lake Chungará (core CHUN11A). Diatoms are grouped according to their habitat and
1007 salinity preferences. Sample scores of the first two axes of Principal Component Analysis
1008 (PCA) and the diatom dissolution index *F* (Flower & Likhoshway, 1993), which varies
1009 between 0 and 1, with values of *F*=1 indicating perfectly preserved valves and *F*=0
1010 indicating that all valves show dissolution, are also plotted. Diatom Assemblage Zones
1011 (DAZs) generated by a broken-stick model of the distribution of variance (Bennett, 1996)

and main lithological units and sedimentary facies according to Sáez et al. (2007) are also shown.

Figure 4.- Principal Component Analysis (PCA) ordination biplot of samples (numbers) and diatom taxa (acronyms) in Lake Chungará. Achcon=*Achnanthes conspicua,* Amplib=*Amphora libyca*, Cocpla=*Cocconeis placentula,* Cycand=*Cyclostephanos andinus*, Cyccfand=*Cyclostephanos* cf. *andinus,* Disste=*Discostella stelligera* complex*,* Fracap=*Fragilaria capucina* and varieties*,* Gommin=*Gomphonema minutum,* Navcry=*Navicula cryptotenella,* Navrad=*Navicula radiosa,* Navtri=*Navicula trivialis,* Navven=*Navicula veneta,* Navsem=*Naviculadicta seminulum,* Nittro=*Nitzschia tropica,* Opemut=*Opephora* sp. aff*. mutabilis,* Plalan=*Planothidium lanceolatum,* Staconv=*Staurosira construens* aff*. venter,* Staconc=*Staurosira construens* f*. construens,* Stacons=*Staurosira construens* f*. subsalina,* Stapin=*Staurosirella pinnata,* Ulnuln=*Ulnaria ulna*

Figure 5.- Diatom and geochemical productivity-related proxies from core CHUN11A, with indications of defined productivity stages and water level phases/events according to the constructed lake-level curve. Data are compared with the water availability curve of Giralt et al. (2008) and the insolation curve in austral summer at 18ºS for the studied period (Berger & Loutre, 1991). Proxies include sample scores for axis 1 (PC1) and axis 2 (PC2) of Principal Component Analysis of the diatom assemblages, percent of benthic diatoms, total biogenic silica (TBSi), total organic carbon (TOC), the TOC/total nitrogen atomic ratio (TOC/TN), and total inorganic carbon (TIC). TBSi and TOC are expressed as percent contents and mass accumulation rates (MARs). The figure also plots values of carbon and nitrogen isotopes in organic matter ($\delta^{13}C_{org}$, $\delta^{15}N_{org}$) and carbonates ($\delta^{18}O_{carbonate}$, $\delta^{13}C_{carbonate}$) (Pueyo et al., 2011), diatom frustules ($\delta^{18}O_{diat}$, $\delta^{13}C_{diat}$) (Hernández et al., 2013), as well as the abundance of the chlorophycean *Botryococcus braunii* (Saéz et al., 2007). All data are plotted against age (cal yr BP).

1038 **Figure 6.-** Sedimentary and paleoecological model for Lake Chungará evolution in the period from
1039 12,400 to 1,300 cal yr BP, with a description of the defined paleoproductivity stages. See
1040 the detailed explanation in the text.

DIATOM ASSEMBLAGE ZONE Depth (cm) Age (cal yr BP)	MAIN TAXA	OVERALL TRENDS
CHUN11-01 860.7 - 835.2 12,400 – 12,100	Dominated by *Cyclostephanos andinus* and *Staurosira construens* aff. *venter*. Other tychoplanktonic (mainly *Fragilaria capucina* and varieties) and benthic (mainly *Nitzschia tropica*, *Cocconeis placentula* and *Opephora* sp. aff *mutabilis*) taxa appear in the record	Codominance of benthic and planktonic diatoms in a oligosaline waterbody of shallow but open waters
CHUN11-02 835.2 – 729.5 12,100 – 11,100	The assemblage is dominated by fluctuating numbers of diatoms of the *Discostella stelligera* complex (26.3 – 87.4%) with *Cyclostephanos andinus*, *Cyclostephanos* cf. *andinus* and the tychopelagic *Staurosira construens* aff. *venter* as subdominant taxa	Shift to deeper and predominantly low mixing water conditions
CHUN11-03 729.5 – 627.9 11,100 – 10,450	*Cyclostephanos andinus* is the dominant taxa, reaching its maximum value (89.2%). The *Discostella stelligera* complex dissapears, except in the interval 693.9 – 683.8 cm. *Cyclostephanos* cf. *andinus* shows episodic peaks. Moderate increase of the subdominant *Staurosira construens* aff. *venter* and the benthic *Cocconeis placentula*. Decline of *Nitzschia tropica*	Water shallowing with episodes of a strong turbulent regime
CHUN11-04 627.9 – 587.2 10,450 – 10,000	Marked increase of the *Discostella stelligera* complex, dominating almost the entire assemblage (82.6 – 94.2 %). *Cyclostephanos andinus* and *Cocconeis placentula* are a minor component of the zone	Deeper and stable water conditions
CHUN11-05 587.2 – 540.3 10,000 - -9,500	Starts with a sharp increase in *Cyclostephanos andinus*, decreasing afterwards. This decrease is paralleled by an increase in *Cyclostephanos* cf. *andinus*, which dominates the assemblage, and by *Staurosira construens* aff. *venter* and *Cocconeis placentula*. The *Discostella stelligera* complex shows low percentages. Reappearance of *Nitzschia tropica*	Shift to a turbulent regime accompanied by a decrease in water level. Slight salinization
CHUN11-06 540.3 – 344.0 9,500 – 7,400	The *Discostella stelligera* complex dominates almost the entire assemblage (67.1 – 95.3%) reaching a maximum in the whole record. *Cyclostephanos andinus* shows low values (5.0 – 23.4%), and *Cyclostephanos* cf. *andinus* dissapears in the record. *Cocconeis placentula* decreases	Lake deepening with a predominantly non-turbulent regime. The reduction in the oligosaline diatoms points to a salt dilution
CHUN11-07 344.0 – 61.8 7,400 – 2,600	*Cyclostephanos andinus* and the diatoms of the *Discostella stelligera* complex show fluctuating values codominating the assemblage. The epiphytic *Cocconeis placentula* increases	Moderate lake shallowing allowing macrophytic development. Shift to moderate mixing conditions
CHUN11-08 61.8 – 14.3 2,600 – 1,300	Sharp increase in the *Discostella stelligera* complex (74.2 – 87.0%) followed by a decline in *Cyclostephanos andinus*. *Cocconeis placentula* becomes a minor component of the assemblage	Maximum lake level situation, with the development of a predominantly stable water column

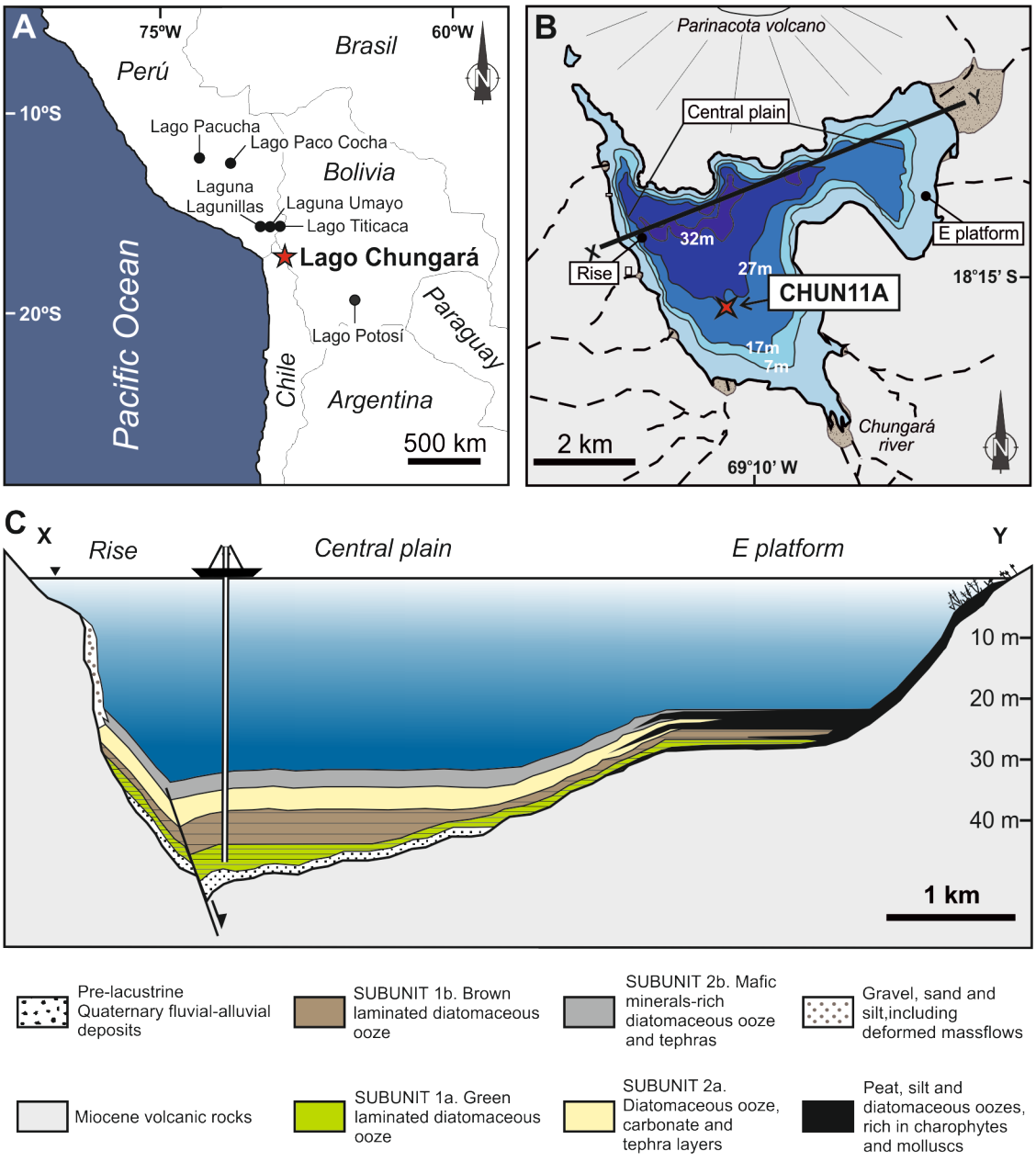
A
75°W
60°W
Brasil
Perú
10°S
Lago Pacucha
Lago Paco Cocha
Bolivia
Laguna Lagunillas
Laguna Umayo
Lago Titicaca
Lago Chungará
20°S
Pacific Ocean
Lago Potosí
Paraguay
Chile
Argentina
500 km
B
Parinacota volcano
Central plain
E platform
Rise
32m
27m
CHUN11A
18°15' S
17m
7m
Chungará river
2 km
69°10' W
C
X
Rise
Central plain
E platform
Y
10 m
20 m
30 m
40 m
1 km
Pre-lacustrine Quaternary fluvial-alluvial deposits
SUBUNIT 1b. Brown laminated diatomaceous ooze
SUBUNIT 2b. Mafic minerals-rich diatomaceous ooze and tephras
Gravel, sand and silt,including deformed massflows
Miocene volcanic rocks
SUBUNIT 1a. Green laminated diatomaceous ooze
SUBUNIT 2a. Diatomaceous ooze, carbonate and tephra layers
Peat, silt and diatomaceous oozes, rich in charophytes and molluscs

Figure 1

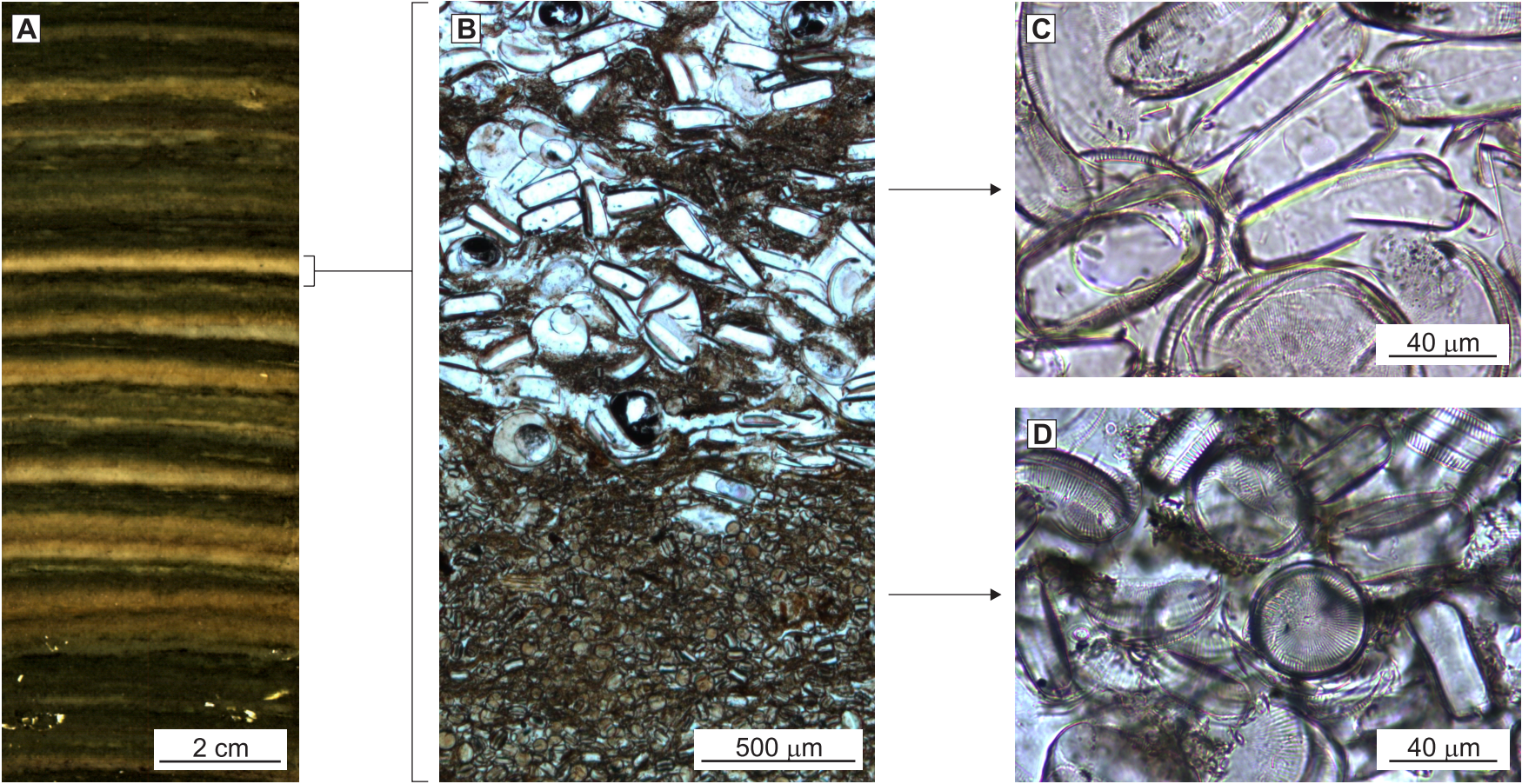

Figure 2

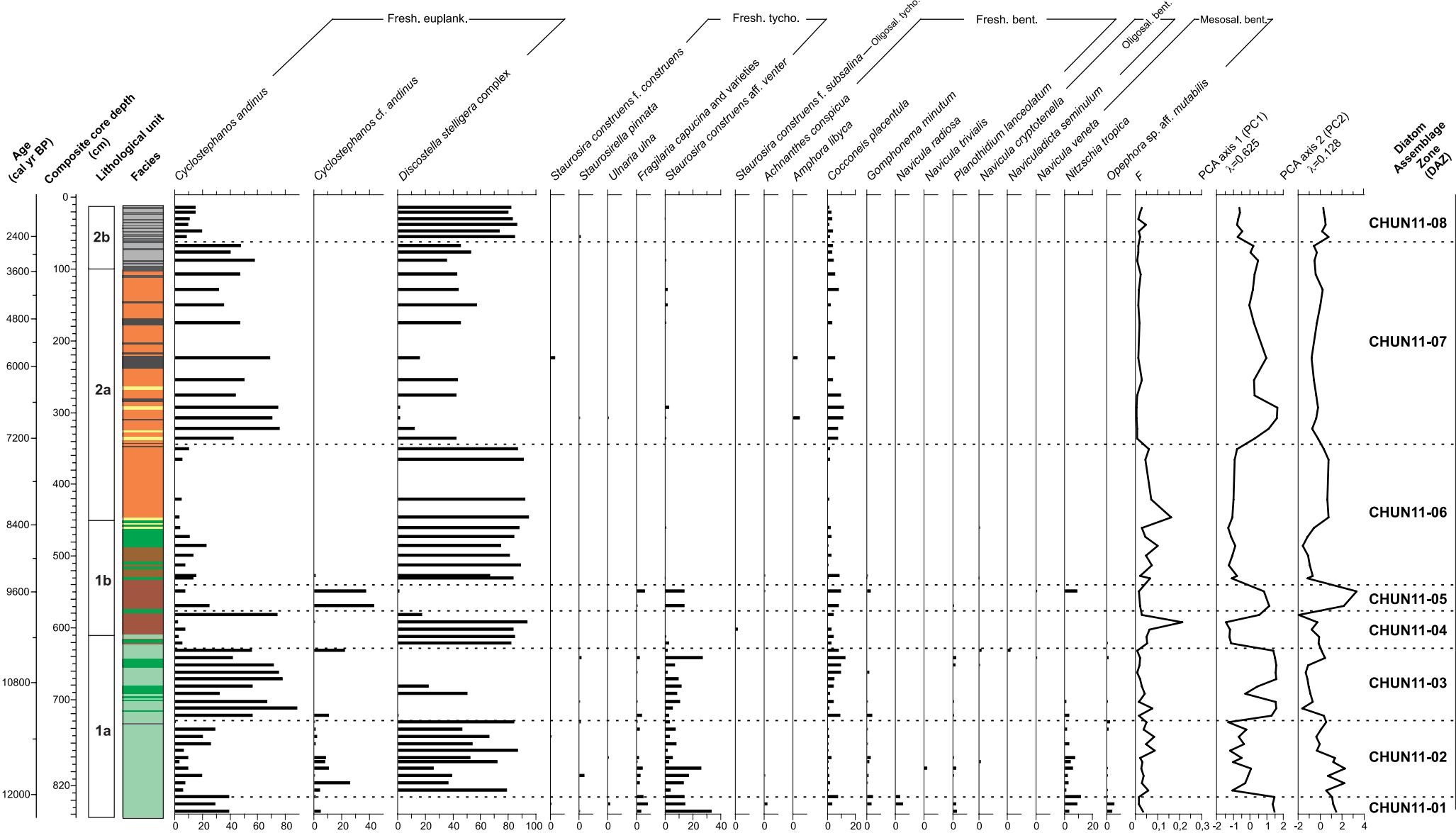
Fresh. euplank.
Fresh. tycho.
Oligosal. tycho.
Fresh. bent.
Oligosal. bent.
Mesosal. bent.
Age (cal yr BP)
Composite core depth (cm)
Lithological unit
Facies
Cyclostephanos andinus
Cyclostephanos cf. andinus
Discostella stelligera complex
Staurosira construens f. construens
Staurosirella pinnata
Ulnaria ulna
Fragilaria capucina and varieties
Staurosira construens aff. venter
Staurosira construens f. subsalina
Achnanthes conspicua
Amphora libyca
Cocconeis placentula
Gomphonema minutum
Navicula radiosa
Navicula trivialis
Planothidium lanceolatum
Navicula cryptotenella
Naviculadicta seminulum
Navicula veneta
Nitzschia tropica
Opephora sp. aff. mutabilis
F
PCA axis 1 (PC1) λ=0.625
PCA axis 2 (PC2) λ=0.128
Diatom Assemblage Zone (DAZ)
2b
2a
1b
1a
CHUN11-08
CHUN11-07
CHUN11-06
CHUN11-05
CHUN11-04
CHUN11-03
CHUN11-02
CHUN11-01
C: Green massive organic-rich facies
B: Brown-white laminated and carbonate-bearing facies
A: Green-White laminated facies
F: Carbonate-rich layers
E: Dark brown to grey banded facies
D: Reddish-to-brown banded and massive facies
N: Grey to white volcaniclastic layers (tephras)

Figure 3

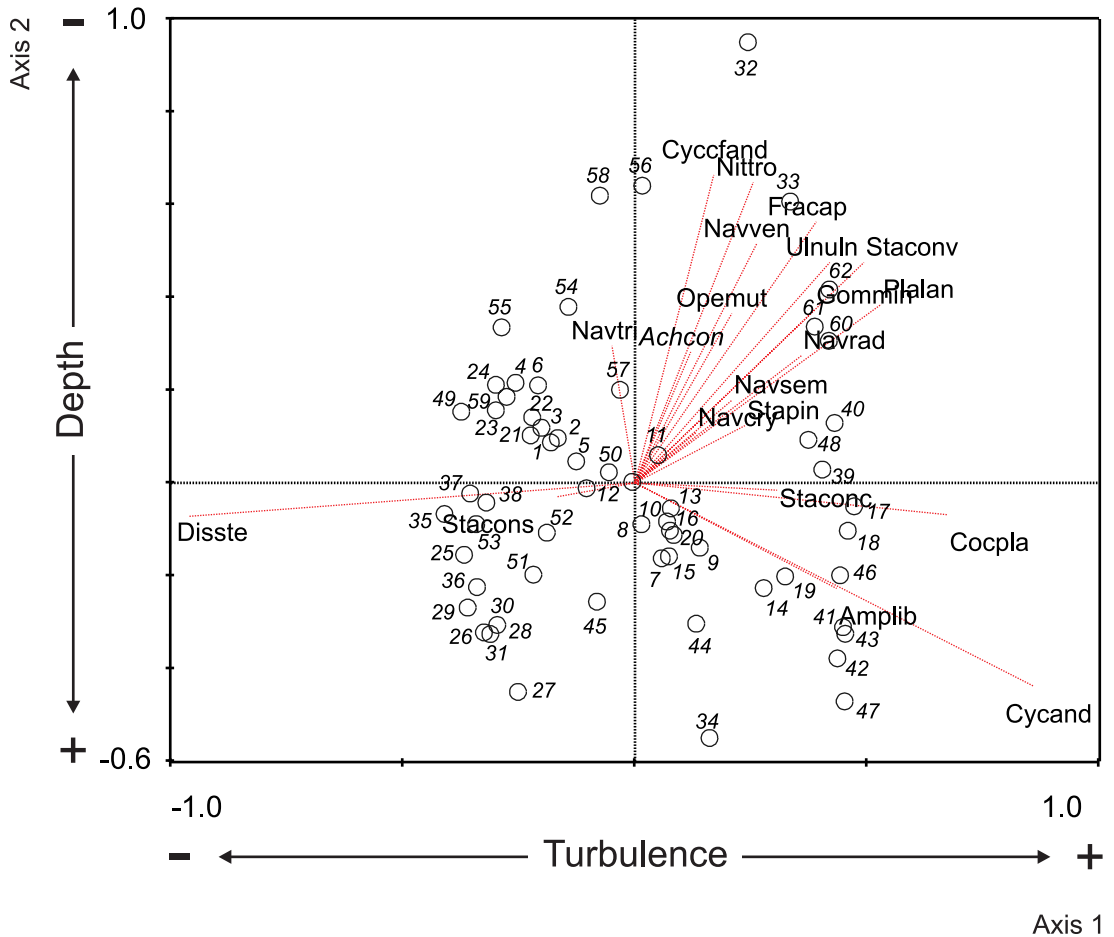
Axis 2
1.0
Depth
-0.6
-1.0
1.0
Turbulence
Axis 1
Cyccfand
Nittro
Fracap
Navven
Ulnuln
Staconv
Opemut
Gommin
Plalan
Navtri
Achcon
Navrad
Navsem
Stapin
Navcry
Staconc
Disste
Stacons
Cocpla
Amplib
Cycand

Figure 4

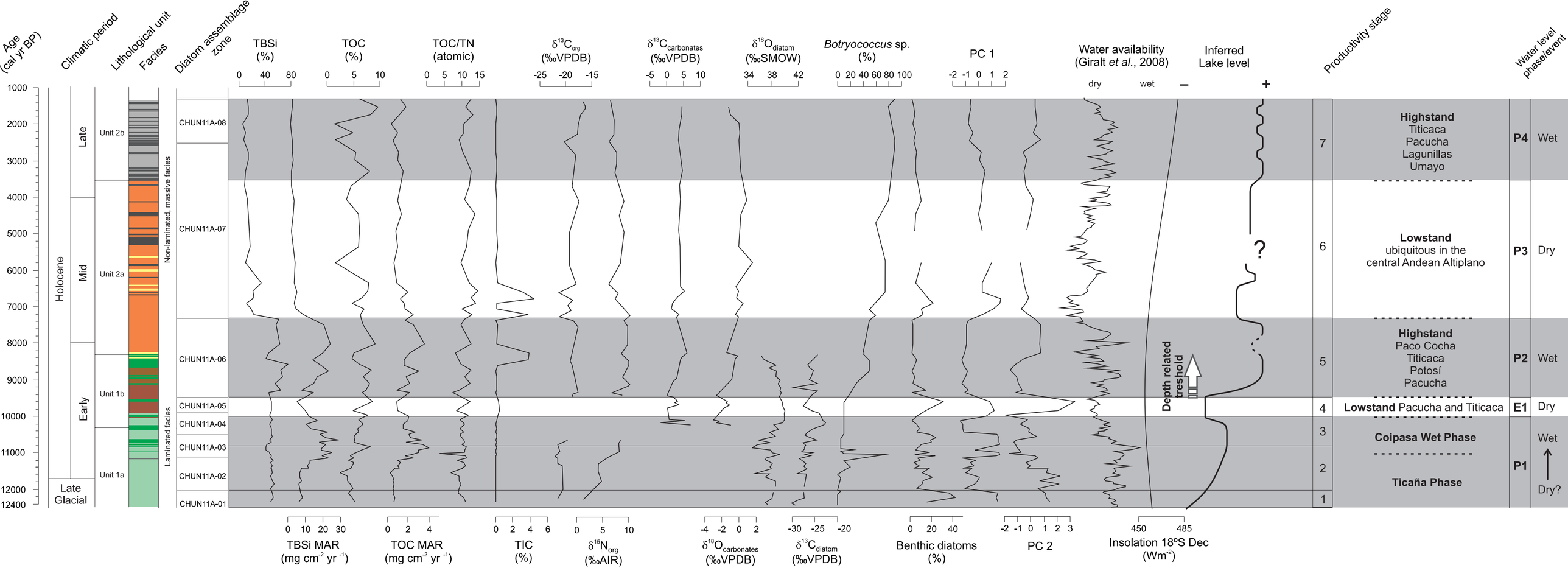
Age (cal yr BP)
Climatic period
Lithological unit
Facies
Diatom assemblage zone
TBSi (%)
TOC (%)
TOC/TN (atomic)
δ13Corg (‰VPDB)
δ13Ccarbonates (‰VPDB)
δ18Odiatom (‰SMOW)
Botryococcus sp. (%)
PC 1
Water availability (Giralt et al., 2008)
dry
wet
Inferred Lake level
Productivity stage
Water level phase/event
Holocene
Late
Mid
Early
Late Glacial
Unit 2b
Unit 2a
Unit 1b
Unit 1a
Non-laminated, massive facies
Laminated facies
CHUN11A-08
CHUN11A-07
CHUN11A-06
CHUN11A-05
CHUN11A-04
CHUN11A-03
CHUN11A-02
CHUN11A-01
Depth related treshold
?
Highstand
Titicaca
Pacucha
Lagunillas
Umayo
Lowstand
ubiquitous in the
central Andean Altiplano
Highstand
Paco Cocha
Titicaca
Potosí
Pacucha
Lowstand Pacucha and Titicaca
Coipasa Wet Phase
Ticaña Phase
P4
P3
P2
E1
P1
Wet
Dry
Wet
Dry?
TBSi MAR (mg cm-2 yr-1)
TOC MAR (mg cm-2 yr-1)
TIC (%)
δ15Norg (‰AIR)
δ18Ocarbonates (‰VPDB)
δ13Cdiatom (‰VPDB)
Benthic diatoms (%)
PC 2
Insolation 18ºS Dec (Wm-2)

Figure 5

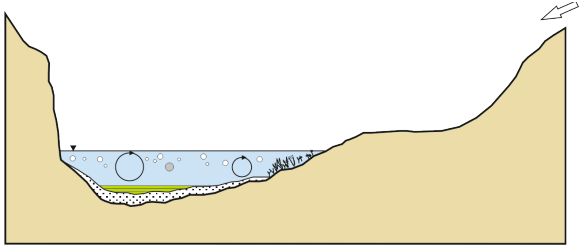

Stage 1 (P1; c. 12,400-12,100 cal yr BP)

- Low productivity by cooling
- Isothermal or quasi-isothermal water column. Well mixed waters

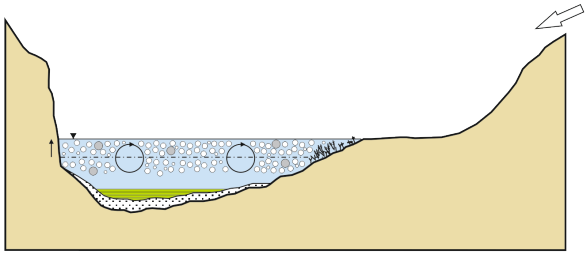

Stage 2 (P1; c. 12,100-10,800 cal yr BP)

- Maximum productivity by warming and increased runoff
- Change from a weak to a well mixed regime

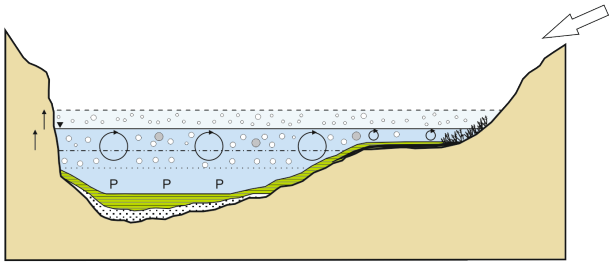

Stage 3 (P1; c. 10,800-10,000 cal yr BP)

- Oligomictic to meromictic condition
- Decreasing productivity by thermal stratification
- Nutrient concentration in the oxygen-depleted hypolimnion

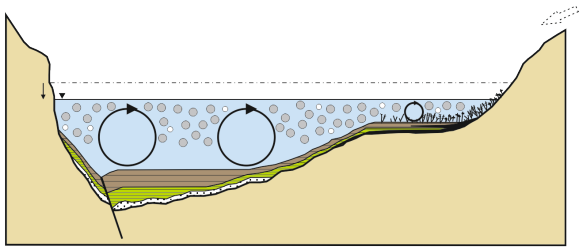

Stage 4 (E1; c. 10,000-9,600 cal yr BP)

- Low productivity by decreased external nutrient upload. Most productivity maintained by internal nutrient supply
- Intermittently well mixed regime

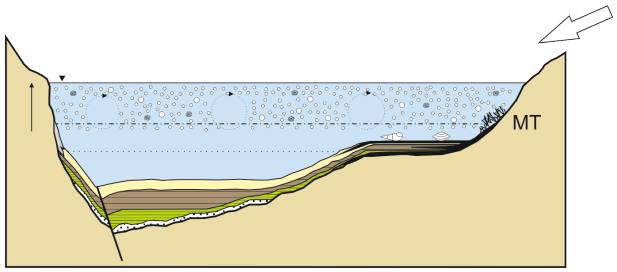

Stage 5 (P2; c. 9,600-7,400 cal yr BP)

- Very high productivity by increased runoff
- Weakly mixed waters
- Depth threshold: internal nutrient supply becomes more restricted. White laminae deposition ceases

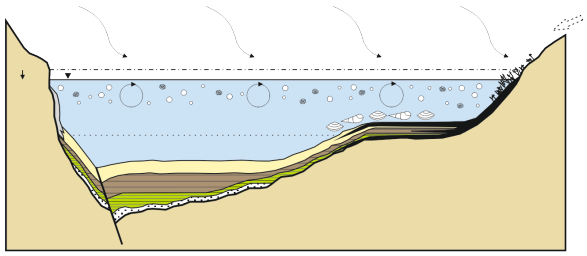

Stage 6 (P3; c. 7,400-3,550 cal yr BP)

- Strong productivity reduction
- Fall in diatom-dominated productivity. Increased relative role of other primary producers
- Likely marked stationality: codominace of weakly mixed with turbulent waters

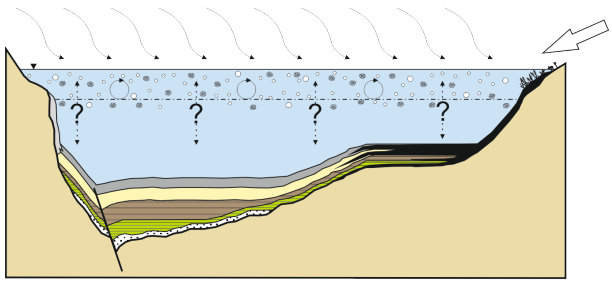

Stage 7 (P4; c. 3,550-1,300 cal yr BP)

- Slight productivity increase by enhanced runoff
- Weakening of the water column mixing regime

Cyclostephanos cf. *andinus*
Cyclostephanos andinus
Discostella stelligera complex
Botryococcus sp.
Macrophytes accumulation
P Phosphorous accumulation
Carbonate accumulation

MT Morphometric threshold
Lake level change
Volcanic ashes fallout
Main lake water level
Secondary lake water level
Former lake water level
Thermocline

High external input
Low external input
Strong mixing
Weak mixing

Figure 6